

Relating spin-foam to canonical loop quantum gravity by graphical calculus

Jinsong Yang^a Cong Zhang^b Yongge Ma^{1c}

^a*School of Physics, Guizhou University, Guiyang 550025, China*

^b*Faculty of Physics, University of Warsaw, Pasteura 5, 02-093 Warsaw, Poland*

^c*Department of Physics, Beijing Normal University, Beijing 100875, China*

E-mail: jsyang@gzu.edu.cn, Cong.Zhang@fuw.edu.pl, mayg@bnu.edu.cn

ABSTRACT:

The graphical calculus method is generalized to study the relation between covariant and canonical dynamics of loop quantum gravity. On one hand, a graphical derivation of the partition function of the generalized Euclidean EPRL spin-foam model is presented. On the other hand, the action of a Euclidean Hamiltonian constraint operator on certain spin network states is calculated by graphical method. It turns out that the EPRL model can provide a rigging map such that the Hamiltonian constraint operator is weakly satisfied on certain physical states for the Immirzi parameter $\beta = 1$. In this sense, the quantum dynamics between the covariant and canonical formulations are consistent to each other.

¹Corresponding author.

Contents

1	Introduction	1
2	The partition function in SFM	3
2.1	The graphical calculus	5
2.2	The partition function in non-boundary cases	11
2.3	The partition function in cases with boundaries	17
3	Matrix elements of a Hamiltonian constraint operator	21
4	Relation in quantum dynamics	25
5	Summary and discussion	31

1 Introduction

Loop quantum gravity (LQG) provides a nonperturbative and background-independent approach to the quantization of general relativity (GR). In the past thirty years, remarkable achievements have been made in the field of LQG (see [1–3] for books, and [4–10] for review articles). Both the canonical and the covariant (path integral) formulations of LQG have been developed.

Canonical LQG is based on the Hamiltonian formulation of GR in the Ashtekar-Barbero variables [11–13]. The spacetime manifold has the structure $M \cong \mathbb{R} \times \Sigma$ with Σ being a 3-dimensional manifold of arbitrary topology. The canonical variables defined on Σ are the $su(2)$ -valued connection $A_a^i(x)$ and the densitized triad $\tilde{E}_i^a(x)$, where $i, j, k, \dots = 1, 2, 3$ are the $su(2)$ indices while a, b, c are the spatial indices. The only nontrivial Poisson bracket between these variables reads

$$\{A_a^i(x), \tilde{E}_j^b(y)\} = \kappa \beta \delta_a^b \delta_j^i \delta^3(x, y), \quad (1.1)$$

where $\kappa \equiv 8\pi G$ with G being the Newtonian constant, and β denotes the Immirzi parameter [13, 14]. The elementary algebra, which can be directly promoted to that of the fundamental operators, consists of the holonomies $g_e(A)$ of A_a^i along one-dimensional edges e and fluxes $\tilde{E}_j(S)$ of \tilde{E}_i^a through two-dimensional surfaces S . It turns out that there is a unique gauge and diffeomorphism invariant cyclic representation of the holonomy-flux C^* -algebra [15]. The resulting representation space is the gauge and diffeomorphism invariant version of the kinematical Hilbert space $\mathcal{H}_{\text{kin}} := L^2(\bar{\mathcal{A}}, d\mu_o)$, where $\bar{\mathcal{A}}$ is the space of distributional connections, and $d\mu_o$ is the Ashtekar-Lewandowski measure [16, 17]. The basis of \mathcal{H}_{kin} consists of the spin network states $T_{\gamma, j, i}(A)$ defined on arbitrary finite graphs γ in Σ with a spin j_e and an intertwiner i_v coloring each edge e and each vertex v of γ . The classical spatial geometric functions, such as the length, area, and volume have been successfully quantized

as the corresponding operators in \mathcal{H}_{kin} , and they all have discrete spectra [18–23]. In the connection formulation, GR is casted into a constrained system with three first-class constraints, the Gaussian, diffeomorphism and Hamiltonian constraints. The Gaussian and diffeomorphism constraints have been successfully implemented at quantum level. Thus the quantum dynamics is encoded in the Hamiltonian constraint. How to suitably quantize the Hamiltonian constraint and how to construct the physical Hilbert space are still under debate. Thus the quantum dynamics in canonical LQG remains obscure up to now. Nevertheless, some well-defined Hamiltonian constraint operators for pure gravity as well as gravity coupled to matters were constructed in different ways [24–31]. Some properties of certain Hamiltonian operators were studied analytically as well as numerically [32–35].

As a kind of path-integral formalism for GR, covariant LQG is well known as certain spin-foam model (SFM). A spin-foam is a dual 2-cell complex Δ^* with faces f labeled by spins j_f and edges e labeled by intertwiners i_e . A slice of a spin-foam at “fixed time” gives a spin network state. Hence a spin-foam can be interpreted as an evolutionary history of a spin network state, and can be understood as a formulation describing the quantum geometry of spacetime. A SFM is defined by assigning transition amplitudes A_f , A_e and A_v to the faces $f \in \Delta^*$, the edges $e \in \Delta^*$ and the vertices $v \in \Delta^*$, respectively. The key observation of current SFMs is that 4-dimensional GR can be written as a BF theory with the so-called the simplicity constraint forcing the B field to be obtained from the tetrad field. Hence the strategy is first to derive the BF partition function $\mathcal{Z}^{\text{BF}}(\Delta^*)$ by discretizing the BF action on Δ^* and its dual Δ , and then to impose a quantum version of the discretized simplicity constraint on $\mathcal{Z}^{\text{BF}}(\Delta^*)$, leading to the resulting partition function

$$\mathcal{Z}^{\text{SFM}}(\Delta^*) = \sum_{j_f, i_e} \prod_f A_f \prod_e A_e \prod_v A_v. \quad (1.2)$$

Different implementing schemes of the simplicity constraint lead to different SFMs, for examples, the Barrett-Crane (BC) model [36, 37], the Engle-Pereira-Rovelli-Livine (EPRL) model [38], and the Freidel-Krasnov (FK) model [39]. The advantage of EPRL model and FK model is that they have correct classical limit to certain sense. The essential difference between the two models and BC model is that the simplicity constraint restrains BF action to the Holst action in the formers but to the Palatini action in the latter. The simplicity constraint was implemented differently in EPRL and FK models. In the former it was imposed at quantum level by the master-constraint criterion [38] or the Gupta-Bleuler criterion [40], while in the latter it was imposed as a semiclassical condition on the coherent state basis proposed by Livine and Speziale [41]. The two models share the same vertex amplitude for $\beta \leq 1$, but differ for $\beta > 1$. Furthermore, the EPRL model was successfully generalized to the Kamiński-Kisielowski-Lewandowski (KKL) model [42, 43], which allows arbitrary boundary graphs.

Whether the dynamics of covariant formulation is equivalent to that of canonical formulation is still an open issue in LQG up to now. Fortunately, the EPRL model generalized by KKL to arbitrary boundary graphs, supporting the quantum states of canonical LQG, has opened a door to set up the relation between the two formulations. Actually, it was shown in Ref. [32] that the rigging map defined by the transition amplitude of EPRL SFM can give certain physical states of the quantum Euclidean Hamiltonian constraint $\hat{H}_T^{\text{E}}(N)$ of canonical LQG proposed by Thiemann in [24] for $\beta = 1$

in the sense that the matrix elements of $\hat{H}_T^E(N)$ vanish. This implies a consistency of the quantum dynamics between covariant and canonical formulations for these states. The aim of this paper is to check whether such a consistency exists also between the EPRL SFM and the Hamiltonian constraint operator proposed in [26] for canonical LQG. We will consider only the Euclidean part of the Hamiltonian constraint in [26] and generalize the graphical calculus presented in [44], which is based on the original Brink's graphical method, to deal with the explicit computations including the SFM. The graphical calculus has been systematically applied to canonical LQG with the virtues of concise and visual formulas, providing a powerful technique for simplifying the complicated calculations [21, 44–46]. Our results show that the rigging map of the Euclidean EPRL model with $\beta = 1$ generalized to arbitrary boundary graphs does give certain physical states for the Euclidean Hamiltonian constraint operator defined in [26] with a special factor ordering, in the same sense as in Ref. [32].

The rest of this paper is organized as follows. In Sec. 2, we give a detailed and concise derivation of the partition function of the generalized Euclidean EPRL model by the graphical calculus, in parallel with the algebraic derivation in [43]. In Sec. 3, we graphically calculate the action of the Euclidean Hamiltonian constraint operator defined in [26] with a special factor ordering on the spin network states ψ_i with a 4-valent vertex v , and obtain its matrix elements. In Sec. 4, we show for $\beta = 1$ that the rigging map of generalized Euclidean EPRL model can provide certain physical states of the Euclidean Hamiltonian constraint operator in [26] such that its matrix elements vanish. In this sense, the quantum dynamics between covariant and canonical LQG are again consistent for these states. Our results are summarized and discussed in Sec. 5.

2 The partition function in SFM

In this section, we will give a concise graphical derivation of the partition function for the Euclidean EPRL model generalized by KKL. The starting point of SFMs is the fact that classical GR can be recasted as a constrained BF theory. Thus the strategy is to firstly derive the partition function of BF theory, and then to impose the simplicity constraint in a satisfactory manner. The partition function of BF theory with gauge group $SO(4)$ or $Spin(4)$ for the Euclidean case in 4-dimensions reads [1, 2, 10]

$$\mathcal{Z}^{BF}(M) = \int dA dB e^{i \int_M \text{Tr}[B \wedge F(A)]} = \int dA \prod_{x \in M} \delta[F(A)], \quad (2.1)$$

where B is a $so(4)$ -valued 2-form field on the spacetime manifold M , F is the curvature of the $so(4)$ connection A on M , the trace Tr is with respect to the Cartan-Killing metric on $so(4)$, and in the second step a formal integration over B field leads to a Dirac delta function. To give a precise meaning to the formal expression (2.1), one needs to discretize M and employ its discrete structure.

Suppose M can be discretized by an arbitrary oriented 2-cell complex Δ . We refer to Refs. [8, 42, 43, 47] for the definition of 2-cell complex. The dual 2-cell complex Δ^* of Δ consists of 2-dimensional faces $f \in \Delta^*$, 1-dimensional edges $e \in \Delta^*$ and 0-dimensional vertices $v \in \Delta^*$. Denote by ∂f the cyclically ordered set of edges bounding the face f and the set of vertices bounding the boundary edges of f , by ∂e the set of faces bounded by e , and by ∂v the set of edges bounded by v and

the set of faces containing v in their boundaries. For Δ^* with a boundary $\partial\Delta^*$, we mean that $\partial\Delta^*$ is a 1-cell complex, called the global boundary graph $\gamma \equiv \partial\Delta^*$, such that it is closed and does not contain any vertex of Δ^* . An edge $e \in \partial\Delta^*$ is called an external edge (link) and it is contained in only one face. A vertex $v \in \partial\Delta^*$ is called an external vertex (node) and it is contained in exactly one internal edge of Δ^* . Given an internal vertex $v \in \Delta^*$, the local boundary graph γ_v of v is the intersection between Δ^* and a small sphere surrounding v . The edges (links) of γ_v are the intersections of $f \in \partial v$ with the sphere, denoted by fv , and the orientations of the edges are induced by those of f . The vertices (nodes) of γ_v are the intersections of $e \in \partial v$ with the sphere. A spin-foam \mathcal{F} is a triple $(\Delta^*, \vec{\rho}, \vec{i})$ consisting of Δ^* , a collection $\vec{\rho}$ of irreducible representations ρ_f of $\text{Spin}(4)$ assigned for each face $f \in \Delta^*$, and a collection \vec{i} of intertwiners i_e associated to each edge $e \in \Delta^*$. A SFM based on a spin-foam is defined by an assignment of the amplitudes A_f, A_e and A_v associated to the internal faces $f \in \Delta^*$, edges $e \in \Delta^*$ and vertices $v \in \Delta^*$. In the case that Δ^* has a boundary $\gamma \cup \gamma'$, a SFM contains also the boundary transition amplitude from the spin network state on γ to the one on γ' .

The partition function \mathcal{Z}^{BF} on Δ^* can be discretized. Given a Δ^* of M , approximating the curvatures $F(A)$ by holonomies $g_{\partial f} = \prod_{e \in \partial f} g_e$ around the loops ∂f composed by the cyclically ordered sets of edges bounding the faces f , and replacing dA by the Haar measure dg_e on $\text{Spin}(4)$, the discretized BF partition function corresponding to Eq. (2.1) is defined by [32, 33, 43]

$$\begin{aligned}
\mathcal{Z}^{\text{BF}}(\Delta^*) &:= \int dg_e \prod_{f \in \Delta^*} \delta \left(\prod_{e \in \partial f} g_e g_l \right) \\
&= \int dg_{ve} \int dg_{fv} \prod_{f \in \Delta^*} \delta \left(\prod_{v \in \partial f} g_{fv} g_{ev'} g_l g_{v''e''} \right) \prod_{fv} \delta(g_{e'v} g_{ve} g_{fv}^{-1}) \\
&= \int dg_{fv}^+ \int dg_{ve}^+ \prod_{f \in \Delta^*} \sum_{j_f^+} d_{j_f^+} \text{Tr}_{j_f^+} \left(\prod_{v \in \partial f} g_{fv}^+ g_{ev'}^+ g_l^+ g_{v''e''}^+ \right) \prod_{fv} \sum_{j_{fv}^+} d_{j_{fv}^+} \text{Tr}_{j_{fv}^+} (g_{e'v}^+ g_{ve}^+ g_{fv}^+)^{-1} \\
&\quad \times \int dg_{fv}^- \int dg_{ve}^- \prod_{f \in \Delta^*} \sum_{j_f^-} d_{j_f^-} \text{Tr}_{j_f^-} \left(\prod_{v \in \partial f} g_{fv}^- g_{ev'}^- g_l^- g_{v''e''}^- \right) \prod_{fv} \sum_{j_{fv}^-} d_{j_{fv}^-} \text{Tr}_{j_{fv}^-} (g_{e'v}^- g_{ve}^- g_{fv}^-),
\end{aligned} \tag{2.2}$$

where g_e denote holonomies along internal edges $e \in \partial f$ with orientations induced by f , g_l denote holonomies along boundary edges $l = f \cap \partial\Delta^*$ with orientations induced by f in the case that Δ^* has a boundary and we set $g_l = \mathbb{I}_G$ in the case that Δ^* has no boundary, in the second step, we split each internal edge e bounded by v and v' into two segments ve and ev' with the same orientation as that of e , and regrouped the groups on segments of internal edges associated to v, ev' and $v''e''$ denote the two segments attaching to the beginning point $v' = b(l)$ and the final point $v'' = f(l)$ of a boundary edge l , in the third step, we used the fact of $\text{Spin}(4) \cong SU(2) \times SU(2)$ which allows us to expand the delta functions on $g \in \text{Spin}(4)$ in terms of irreducible representations (j^+, j^-) of $(g^+, g^-) \in SU(2) \times SU(2)$ as

$$\delta(g) = \delta(g^+) \delta(g^-) = \sum_{j^+} d_{j^+} \text{Tr}_{j^+}(g^+) \sum_{j^-} d_{j^-} \text{Tr}_{j^-}(g^-), \tag{2.3}$$

with $d_j := 2j + 1$ being the dimension of the representation space \mathcal{H}_j of $SU(2)$.

To further derive the partition function $\mathcal{Z}^{\text{SFM}}(\Delta^*)$ of a SFM for GR from $\mathcal{Z}^{\text{BF}}(\Delta^*)$, one takes the following procedure [43]. First, integrating out the group elements g_{ve}^\pm associated to the internal edges of Δ^* reduces the integrand in $\mathcal{Z}^{\text{BF}}(\Delta^*)$ into a function $\prod_f A_f^{\text{BF}}(\{g_{fv}^+, g_{fv}^-; g_l^+, g_l^-\})$. Second, the quantum simplicity constraint is imposed in a suitable way on the Hilbert spaces \mathcal{H}_{γ_v} associated to all (local) vertex-boundary graphs γ_v and on the Hilbert spaces $\mathcal{H}_{\partial\Delta^*}$ associated to the (global) boundary graphs $\partial\Delta^*$ for Δ^* with a boundary. This will further restrict $A_f^{\text{BF}}(\{g_{fv}^+, g_{fv}^-; g_l^+, g_l^-\})$ to $A_f^{\text{SFM}}(\{g_{fv}^+, g_{fv}^-; g_l\})$. Implementing the simplicity constraint in different manners results in different SFMs. Finally, for each internal vertex $v \in \Delta^*$, one performs the integration over the group elements g_{fv}^\pm associated to γ_v . Then the resulting partition function $\mathcal{Z}^{\text{SFM}}(\Delta^*)$ will be expressed as a sum over representations and intertwiners. Note that a derivation of the partition function by a procedure alternative to the above one was presented in [10].

2.1 The graphical calculus

In this subsection, we briefly recall the elements of the Brink's graphical calculus applied in canonical LQG (see [44, 45] for details), and then extend it to compute the integral over the product of irreducible representations of $SU(2)$ in order to derive $\mathcal{Z}^{\text{SFM}}(\Delta^*)$. We will focus on the graphical representations of the matrix elements of holonomies g_e associated to edges e , the intertwiners i_v associated to vertices v , and the graphical transformation rules.

The intertwiner is closely related to the $3j$ -symbol, which is graphically represented by an oriented node with three black lines labeled by three angular momenta and a sign factor as

$$\begin{pmatrix} j_1 & j_2 & j_3 \\ m_1 & m_2 & m_3 \end{pmatrix} = m_1 \text{---} j_1 \text{---} \begin{array}{c} j_3 \nearrow \\ + \\ j_2 \searrow \end{array} \begin{array}{c} m_3 \\ m_2 \end{array} = m_1 \text{---} j_1 \text{---} \begin{array}{c} j_2 \nearrow \\ - \\ j_3 \searrow \end{array} \begin{array}{c} m_2 \\ m_3 \end{array}, \quad (2.4)$$

where the sign $-$ (or $+$) denotes the clockwise (or counter-clockwise) orientation of the node with the cyclic order of the lines. A rotated diagram represents the same $3j$ -symbol as the initial diagram, and the angles between two lines as well as the lengths of lines have no significance. A special $3j$ -symbol with one zero-valued angular momentum is related to the “metric” tensor $C_{mm'}^{(j)}$ graphically by

$$m' \text{---} j' \text{---} \begin{array}{c} 0 \nearrow \\ + \\ j \searrow \end{array} = \frac{\delta_{j,j'}}{\sqrt{d_j}} m' \text{---} \begin{array}{c} j \end{array} \text{---} m, \quad (2.5)$$

where a black line with an arrow on it graphically represents the “metric” tensor

$$C_{mm'}^{(j)} = (-1)^{j-m'} \delta_{m,-m'} = (-1)^{j+m} \delta_{m,-m'} = m' \text{---} \begin{array}{c} j \end{array} \text{---} m. \quad (2.6)$$

The “metric” tensor $C_{mm'}^{(j)}$ on \mathcal{H}_j often occurs in the contraction of two $3j$ -symbols with the same j values. The inverse $C_{(j)}^{m'm}$ can be expressed by

$$C_{(j)}^{m'm} = (-1)^{j-m'} \delta_{m,-m'} = (-1)^{j+m} \delta_{m,-m'} = m' \text{---} \begin{array}{c} j \end{array} \text{---} m. \quad (2.7)$$

A black line denoted by j without arrow on it represents the Kronecker delta in \mathcal{H}_j , i.e.,

$$\delta^{(j)m}_{m'} = \text{---} \overset{j}{\text{---}} \text{---} \text{---} m'. \quad (2.8)$$

The contraction of a $3j$ -symbol with a “metric” represents the Clebsch-Gordan coefficient multiplied by a factor. In graphical representation, summation over the magnetic quantum numbers m is represented by joining the free ends of the corresponding lines. Hence graphically the contraction of a $3j$ -symbol with a “metric” is represented by a node with one arrow as

$$\begin{array}{c} m_1 \quad m_2 \\ | \quad | \\ j_1 \quad j_2 \\ \text{---} \quad \text{---} \\ \text{---} \quad \text{---} \\ \quad \quad \quad j_3 \end{array} m_3 = \begin{pmatrix} j_1 & j_2 & j_3 \\ m_1 & m_2 & m_3 \end{pmatrix} C_{(j_3)}^{m_3 m_3} = \frac{(-1)^{j_1-j_2-j_3}}{\sqrt{d_{j_3}}} \langle j_3 m_3 | j_1 m_1 j_2 m_2 \rangle, \quad (2.9)$$

which is the building block in the construction of an intertwiner. Notice that the intertwiner is defined up to a factor with norm 1. The normalized intertwiner i_v associated to a vertex v , from which n edges with n spins j_1, \dots, j_n start, is defined by [44]

$$\begin{aligned} (i_v^{J;\vec{d}})_{m_1 m_2 \dots m_n}^M &\equiv (i_{j_1 \dots j_n}^{J;\vec{d}})_{m_1 m_2 \dots m_n}^M \\ &:= (-1)^{j_1 - \sum_{i=2}^n j_i - J} \langle JM; \vec{d} | j_1 m_1 j_2 m_2 \dots j_n m_n \rangle \\ &= (-1)^{j_1 - \sum_{i=2}^n j_i - J} \sum_{k_2, \dots, k_{n-1}} \langle a_2 k_2 | j_1 m_1 j_2 m_2 \rangle \langle a_3 k_3 | a_2 k_2 j_3 m_3 \rangle \\ &\quad \times \dots \times \langle JM | a_{n-1} k_{n-1} j_n m_n \rangle \\ &= \prod_{i=2}^{n-1} \sqrt{d_{a_i}} \sqrt{d_J} \begin{array}{c} m_1 \quad m_2 \\ | \quad | \\ j_1 \quad j_2 \\ \text{---} \quad \text{---} \\ \text{---} \quad \text{---} \\ \quad \quad \quad a_2 \end{array} \dots \begin{array}{c} m_{n-1} \quad m_n \\ | \quad | \\ j_{n-1} \quad j_n \\ \text{---} \quad \text{---} \\ \text{---} \quad \text{---} \\ \quad \quad \quad a_{n-1} \end{array} \xrightarrow{J} M, \end{aligned} \quad (2.10)$$

which describes the coupling of n angular momenta j_1, \dots, j_n to a total angular momentum J in the standard coupling scheme such that j_1 is firstly coupled to j_2 to give a resultant a_2 , and then a_2 is coupled to j_3 to yield a_3 , and so on. Here $\vec{d} \equiv \{a_2, \dots, a_{n-1}\}$ denotes the set of the angular momenta appeared in the intermediate coupling. The normalized gauge-invariant (or gauge-variant) intertwiner corresponds to the resulting angular momentum $J = 0$ (or $J \neq 0$). For the convenience of graphical calculus considered in this paper, we specify the normalized gauge-invariant intertwiner associated to a vertex v as

$$\begin{aligned} (i_v^{\vec{d}})_{m_1 m_2 \dots m_n} &:= (-1)^{2j_n} (i_v^{J=0; \vec{d}})_{m_1 m_2 \dots m_n}^{M=0} = (-1)^{2j_n} \prod_{i=2}^{n-1} \sqrt{d_{a_i}} \begin{array}{c} m_1 \quad m_2 \\ | \quad | \\ j_1 \quad j_2 \\ \text{---} \quad \text{---} \\ \text{---} \quad \text{---} \\ \quad \quad \quad a_2 \end{array} \dots \begin{array}{c} m_{n-1} \quad m_n \\ | \quad | \\ j_{n-1} \quad j_n \\ \text{---} \quad \text{---} \\ \text{---} \quad \text{---} \\ \quad \quad \quad a_{n-1} \end{array} \xrightarrow{0} 0 \\ &= \prod_{i=2}^{n-2} \sqrt{d_{a_i}} \begin{array}{c} m_1 \quad m_2 \\ | \quad | \\ j_1 \quad j_2 \\ \text{---} \quad \text{---} \\ \text{---} \quad \text{---} \\ \quad \quad \quad a_2 \end{array} \dots \begin{array}{c} m_{n-1} \quad m_n \\ | \quad | \\ j_{n-1} \quad j_n \\ \text{---} \quad \text{---} \\ \text{---} \quad \text{---} \\ \quad \quad \quad a_{n-2} \end{array}, \end{aligned} \quad (2.11)$$

where in the second step the identities (2.5) and (2.20) (see below) were used. Hence the $3j$ -symbol (2.4) is indeed the normalized gauge-invariant intertwiner associated to a trivalent vertex v from which three edges start. The “metric” tensor (2.6), as the special $3j$ -symbol, is the gauge-invariant intertwiner associated to a divalent vertex v from which two edges start. It can be normalized by multiplying a factor $1/\sqrt{d_j}$. The Kronecker delta (2.8) in \mathcal{H}_j is the gauge-invariant intertwiner associated to

a divalent (trivial) vertex v such that $v = b(e) = f(e')$ is the intersection of two edges e and e' , which can be normalized by multiplying a factor $1/\sqrt{d_j}$.

Now we turn to the graphical transformation rules reflecting the properties of the $3j$ -symbol. The $3j$ -symbol has the following cyclic symmetries. An even permutation of the columns of the $3j$ -symbol keeps its value unchanged, while an odd permutation leads to a multiplication by a factor $(-1)^{j_1+j_2+j_3}$, i.e.,

$$\begin{array}{c} m_1 \text{---} j_1 \text{---} \begin{array}{c} j_3 \nearrow \\ + \\ j_2 \searrow \end{array} \begin{array}{c} m_3 \\ m_2 \end{array} \end{array} = (-1)^{j_1+j_2+j_3} \begin{array}{c} m_1 \text{---} j_1 \text{---} \begin{array}{c} j_2 \nearrow \\ + \\ j_3 \searrow \end{array} \begin{array}{c} m_2 \\ m_3 \end{array} \end{array} = (-1)^{j_1+j_2+j_3} \begin{array}{c} m_1 \text{---} j_1 \text{---} \begin{array}{c} j_3 \nearrow \\ - \\ j_2 \searrow \end{array} \begin{array}{c} m_3 \\ m_2 \end{array} \end{array}. \quad (2.12)$$

The two orthogonality relations for $3j$ -symbols are represented by the graphical rules

$$\sum_j d_j \begin{array}{c} n_1 \text{---} j_1 \text{---} \begin{array}{c} n_2 \nearrow \\ j \\ j_2 \searrow \end{array} \begin{array}{c} m_1 \\ m_2 \end{array} \end{array} = \begin{array}{c} n_1 \\ j_1 \\ m_1 \end{array} \begin{array}{c} n_2 \\ j_2 \\ m_2 \end{array}, \quad (2.13)$$

$$\begin{array}{c} m'_1 \text{---} j'_1 \text{---} \begin{array}{c} j_2 \nearrow \\ + \\ j_3 \searrow \end{array} \begin{array}{c} m_1 \\ m_1 \end{array} \end{array} = \frac{\delta_{j_1, j'_1}}{d_{j_1}} \begin{array}{c} m'_1 \\ j_1 \\ m_1 \end{array}. \quad (2.14)$$

From Eqs. (2.8) and (2.14), one can easily obtain the following two graphical rules

$$j \text{---} \text{---} \text{---} = d_j, \quad (2.15)$$

$$\begin{array}{c} j_1 \nearrow \\ j_2 \searrow \\ j_3 \searrow \end{array} + = 1. \quad (2.16)$$

The rules of reversing, removing and adding arrows in a graph read

$$\begin{array}{c} m_1 \text{---} j_1 \text{---} \begin{array}{c} j_3 \nearrow \\ + \\ j_2 \searrow \end{array} \begin{array}{c} m_3 \\ m_2 \end{array} \end{array} = \begin{array}{c} m_1 \text{---} j_1 \text{---} \begin{array}{c} j_3 \nearrow \\ + \\ j_2 \searrow \end{array} \begin{array}{c} m_3 \\ m_2 \end{array} \end{array} = \begin{array}{c} m_1 \text{---} j_1 \text{---} \begin{array}{c} j_3 \nearrow \\ + \\ j_2 \searrow \end{array} \begin{array}{c} m_3 \\ m_2 \end{array} \end{array}, \quad (2.17)$$

$$m \text{---} \overset{j}{\rightarrow} m' = (-1)^{2j} m \text{---} \overset{j}{\leftarrow} m', \quad (2.18)$$

$$m \text{---} \overset{j}{\leftarrow} m' = m \text{---} \overset{j}{\rightarrow} m' = m \text{---} \overset{j}{\rightarrow} m', \quad (2.19)$$

$$m \text{---} \overset{j}{\rightarrow} m' = m \text{---} \overset{j}{\leftarrow} m' = (-1)^{2j} m \text{---} \overset{j}{\leftarrow} m'. \quad (2.20)$$

These and the following rules are also useful to simplify graphs. A graph is regarded as a block diagram with n external lines if, by rules (2.17)-(2.20), it can be transformed into the form such that every internal line has exactly one arrow and every external line has no arrow. Then the block diagram can be decomposed for different n as follows.

(a) $n = 1$

$$\begin{array}{c} n \\ | \\ j \\ \boxed{} \end{array} = \delta_{j,0} \delta_{n,0} \begin{array}{c} 0 \\ | \\ 0 \\ \boxed{} \end{array} . \quad (2.21)$$

(b) $n = 2$

$$\begin{array}{c} n_1 \quad n_2 \\ | \quad | \\ j_1 \quad j_2 \\ \boxed{} \end{array} = \frac{\delta_{j_1, j_2}}{d_{j_1}} \begin{array}{c} n_1 \quad n_2 \\ \curvearrowright \quad \curvearrowleft \\ j_1 \quad j_1 \\ \boxed{} \end{array} . \quad (2.22)$$

(c) $n = 3$

$$\begin{array}{c} n_1 \quad n_2 \quad n_3 \\ | \quad | \quad | \\ j_1 \quad j_2 \quad j_3 \\ \boxed{} \end{array} = \begin{array}{c} n_1 \quad n_2 \quad n_3 \\ \curvearrowright \quad \curvearrowleft \quad \curvearrowleft \\ j_1 \quad j_2 \quad j_3 \\ \boxed{} \end{array} + \begin{array}{c} n_1 \quad n_2 \quad n_3 \\ \curvearrowleft \quad \curvearrowright \quad \curvearrowleft \\ j_1 \quad j_2 \quad j_3 \\ \boxed{} \end{array} . \quad (2.23)$$

(d) $n > 3$

$$\begin{array}{c} n_1 \quad n_2 \quad \dots \quad n_{n-1} \quad n_n \\ | \quad | \quad \dots \quad | \quad | \\ j_1 \quad j_2 \quad \dots \quad j_{n-1} \quad j_n \\ \boxed{} \end{array} = \sum_{\{a_2, \dots, a_{n-2}\}} \prod_{i=2}^{n-2} d_{a_i} \begin{array}{c} n_1 \quad n_2 \quad \dots \quad n_{n-1} \quad n_n \\ \curvearrowright \quad \curvearrowleft \quad \dots \quad \curvearrowleft \quad \curvearrowleft \\ j_1 \quad j_2 \quad \dots \quad j_{n-1} \quad j_n \\ \boxed{} \end{array} . \quad (2.24)$$

A direct application of Eq. (2.23) yields

$$\begin{array}{c} m_3 \\ | \\ j_3 - \\ | \\ j_5 \\ | \\ j_1 \\ m_1 \end{array} \begin{array}{c} - \\ | \\ j_4 \\ | \\ j_6 \\ | \\ m_2 \end{array} = \begin{array}{c} + \\ | \\ j_5 \\ | \\ j_1 \\ + \end{array} \begin{array}{c} j_3 \\ | \\ j_2 \\ | \\ j_6 \end{array} \begin{array}{c} j_4 \\ | \\ j_2 \\ | \\ j_6 \end{array} + \begin{array}{c} m_3 \\ | \\ j_3 \\ | \\ j_1 \\ m_1 \end{array} \begin{array}{c} j_2 \\ | \\ m_2 \end{array} , \quad (2.25)$$

where the first graph on the right-hand side represents a $6j$ -symbol, i.e.,

$$\begin{array}{c} + \\ | \\ j_5 \\ | \\ j_1 \\ + \end{array} \begin{array}{c} j_3 \\ | \\ j_2 \\ | \\ j_6 \end{array} \begin{array}{c} j_4 \\ | \\ j_2 \\ | \\ j_6 \end{array} = \left\{ \begin{array}{ccc} j_1 & j_2 & j_3 \\ j_4 & j_5 & j_6 \end{array} \right\} , \quad (2.26)$$

which is obtained by contracting four $3j$ -symbols. The $6j$ -symbol is invariant by any permutation of columns and exchange of an upper and a lower arguments in each of column, e.g.,

$$\begin{aligned} \begin{Bmatrix} j_1 & j_2 & j_3 \\ j_4 & j_5 & j_6 \end{Bmatrix} &= \begin{Bmatrix} j_2 & j_1 & j_3 \\ j_5 & j_4 & j_6 \end{Bmatrix} = \begin{Bmatrix} j_3 & j_2 & j_1 \\ j_6 & j_5 & j_4 \end{Bmatrix} = \dots \\ &= \begin{Bmatrix} j_4 & j_5 & j_3 \\ j_1 & j_2 & j_6 \end{Bmatrix} = \begin{Bmatrix} j_4 & j_2 & j_6 \\ j_1 & j_5 & j_3 \end{Bmatrix} = \dots \end{aligned} \quad (2.27)$$

The matrix representation $[\pi_j(g_e)]^m_n$ of holonomy $g_e \equiv g_e(A) \in SU(2)$ of a $su(2)$ -valued connection A along an edge e on Σ is denoted by a colored line (not a black line) with an arrow on it as [44]

$$[\pi_j(g_e)]^m_n = m \xrightarrow[j]{e} n. \quad (2.28)$$

All the information about $[\pi_j(g_e)]^m_n$ have been encoded in the graph in the right hand side of Eq. (2.28). The corresponding irreducible representation π_j of g_e is denoted by e and j labeling the line. The orientation of e with respect to the vertices is reflected by the orientation of the arrow on the line. The row (former or up) index and the column (latter or down) index are denoted by the two indices m and n labeling the starting and the ending points of the line, respectively, and the orientation of the arrow is from its row index m to its column index n . The graphical transformations for the holonomy consist of the following two rules. First, a transformation from the irreducible representation of g_e^{-1} to that of g_e is given by

$$[\pi_j(g_e^{-1})]^n_m = [\pi_j(g_{e^{-1}})]^n_m = C_{mm'}^{(j)} [\pi_j(g_e)]^{m'}_{n'} C_{(j)}^{n'n} = m \xleftarrow[j]{e^{-1}} n = m \xleftarrow[j]{e} n. \quad (2.29)$$

Second, coupling two representations of the same holonomy g_e , corresponding to the Clebsch-Gordan series, is expressed as

$$\begin{aligned} [\pi_{j_1}(g_e)]^{m_1}_{n_1} [\pi_{j_2}(g_e)]^{m_2}_{n_2} &= \begin{array}{c} m_1 \xrightarrow[j_1]{e} m'_1 \\ m_2 \xrightarrow[j_2]{e} m'_2 \end{array} = \sum_{j_3} d_{j_3} \begin{array}{c} m_1 \xrightarrow[j_1+j_3]{e} m'_1 \\ m_2 \xrightarrow[j_2]{e} m'_2 \end{array} \\ &= \sum_{j_3} d_{j_3} \begin{array}{c} m_1 \xrightarrow[j_2]{e} m'_1 \\ m_2 \xrightarrow[j_3]{e} m'_2 \end{array}, \end{aligned} \quad (2.30)$$

which can be easily generalized to

$$\begin{aligned} [\pi_{j_1}(g_e)]^{m_1}_{n_1} [\pi_{j_2}(g_e)]^{m_2}_{n_2} \cdots [\pi_{j_n}(g_e)]^{m_n}_{n_n} &= \begin{array}{c} n_1 \quad n_2 \quad \dots \quad n_{n-1} \quad n_n \\ e \xrightarrow{j_1} e \xrightarrow{j_2} \dots e \xrightarrow{j_{n-1}} e \xrightarrow{j_n} \\ m_1 \quad m_2 \quad \dots \quad m_{n-1} \quad m_n \end{array} \\ &= \sum_{a_2} d_{a_2} \begin{array}{c} n_1 \quad n_2 \quad \dots \quad n_{n-1} \quad n_n \\ e \xrightarrow{j_1} e \xrightarrow{j_2} \dots e \xrightarrow{j_{n-1}} e \xrightarrow{j_n} \\ m_1 \quad m_2 \quad \dots \quad m_{n-1} \quad m_n \end{array} \end{aligned}$$

$$\begin{aligned}
&= \sum_{a_2} d_{a_2} \begin{array}{c} n_1 \quad n_2 \\ j_1 \quad j_2 \\ m_1 \quad m_2 \end{array} \begin{array}{c} - \\ + \end{array} \begin{array}{c} a_2 \\ a_2 \end{array} e \begin{array}{c} j_1 \quad j_2 \\ m_1 \quad m_2 \end{array} \dots \begin{array}{c} n_{n-1} \quad n_n \\ j_{n-1} \quad j_n \\ m_{n-1} \quad m_n \end{array} e \begin{array}{c} j_{n-1} \quad j_n \\ m_{n-1} \quad m_n \end{array} \\
&= \sum_{\{a_2, \dots, a_{n-1}, J\}} \prod_{i=2}^{n-1} d_{a_i} d_J \begin{array}{c} n_1 \quad n_2 \quad \dots \quad n_{n-1} \quad n_n \\ j_1 \quad j_2 \quad \dots \quad j_{n-1} \quad j_n \\ m_1 \quad m_2 \quad \dots \quad m_{n-1} \quad m_n \end{array} \begin{array}{c} - \\ + \end{array} \begin{array}{c} a_2 \\ a_2 \end{array} \dots \begin{array}{c} a_{n-2} \\ a_{n-2} \end{array} \begin{array}{c} a_{n-1} \\ a_{n-1} \end{array} J \begin{array}{c} e \end{array} J.
\end{aligned} \tag{2.31}$$

Now we extend the above graphical calculus to compute the integral over the product of irreducible representations of g_e . By Eq. (2.31), the integral can be evaluated graphically by

$$\begin{aligned}
&\int dg_e [\pi_{j_1}(g_e)]^{m_1}_{n_1} [\pi_{j_2}(g_e)]^{m_2}_{n_2} \dots [\pi_{j_n}(g_e)]^{m_n}_{n_n} \\
&= \int dg_e \begin{array}{c} n_1 \quad n_2 \\ j_1 \quad j_2 \\ m_1 \quad m_2 \end{array} e \begin{array}{c} j_1 \quad j_2 \\ m_1 \quad m_2 \end{array} \dots \begin{array}{c} n_{n-1} \quad n_n \\ j_{n-1} \quad j_n \\ m_{n-1} \quad m_n \end{array} e \begin{array}{c} j_{n-1} \quad j_n \\ m_{n-1} \quad m_n \end{array} \\
&= \sum_{\{a_2, \dots, a_{n-1}, J\}} \prod_{i=2}^{n-1} d_{a_i} d_J \int dg_e \begin{array}{c} n_1 \quad n_2 \quad \dots \quad n_{n-1} \quad n_n \\ j_1 \quad j_2 \quad \dots \quad j_{n-1} \quad j_n \\ m_1 \quad m_2 \quad \dots \quad m_{n-1} \quad m_n \end{array} \begin{array}{c} - \\ + \end{array} \begin{array}{c} a_2 \\ a_2 \end{array} \dots \begin{array}{c} a_{n-2} \\ a_{n-2} \end{array} \begin{array}{c} a_{n-1} \\ a_{n-1} \end{array} J \begin{array}{c} e \end{array} J \\
&= \sum_{\{a_2, \dots, a_{n-2}\}} \prod_{i=2}^{n-2} d_{a_i} \begin{array}{c} n_1 \quad n_2 \quad \dots \quad n_{n-1} \quad n_n \\ j_1 \quad j_2 \quad \dots \quad j_{n-1} \quad j_n \\ m_1 \quad m_2 \quad \dots \quad m_{n-1} \quad m_n \end{array} \begin{array}{c} - \\ + \end{array} \begin{array}{c} a_2 \\ a_2 \end{array} \dots \begin{array}{c} a_{n-2} \\ a_{n-2} \end{array} \\
&= \sum_{\vec{a}} (i_{v_1}^{\vec{a}})_{m_1 \dots m_n} (i_{v_2}^{\vec{a}})^{n_1 \dots n_n},
\end{aligned} \tag{2.32}$$

where we used $\int dg_e [\pi_J(g_e)]^M_N = \delta_{J,0} \delta^{M,0} \delta_{N,0}$, the identities (2.5), (2.20) and $(-1)^{4j_n} = 1$ in the third step. Thus the integration over all group elements associated to e gives two normalized gauge-invariant intertwiners i_{v_1} and i_{v_2} to the two vertices (endpoints) v_1 and v_2 of e . Similarly, one has the following useful formulas.

(a) $n = 2$

$$\int dg_e \begin{array}{c} n_1 \quad n_2 \\ j_1 \quad j_2 \\ m_1 \quad m_2 \end{array} e \begin{array}{c} j_1 \quad j_2 \\ m_1 \quad m_2 \end{array} = \frac{\delta_{j_1, j_2}}{d_{j_1}} \begin{array}{c} n_1 \quad n_2 \\ j_1 \quad j_1 \\ m_1 \quad m_2 \end{array} = \frac{\delta_{j_1, j_2}}{d_{j_1}} \begin{array}{c} n_1 \quad n_2 \\ j_1 \quad j_1 \\ m_1 \quad m_2 \end{array}, \tag{2.33}$$

$$\int dg_e \begin{array}{c} n_1 \quad n_2 \\ j_1 \quad j_2 \\ m_1 \quad m_2 \end{array} e \begin{array}{c} j_1 \quad j_2 \\ m_1 \quad m_2 \end{array} e^{-1} \begin{array}{c} j_1 \quad j_2 \\ m_1 \quad m_2 \end{array} = \frac{\delta_{j_1, j_2}}{d_{j_1}} \begin{array}{c} n_1 \quad n_2 \\ j_1 \quad j_1 \\ m_1 \quad m_2 \end{array}. \tag{2.34}$$

(b) $n = 3$

$$\int dg_e \begin{array}{c} n_1 \\ | \\ e \leftarrow j_1 \\ | \\ m_1 \end{array} \begin{array}{c} n_2 \\ | \\ e \leftarrow j_2 \\ | \\ m_2 \end{array} \begin{array}{c} n_3 \\ | \\ e \leftarrow j_3 \\ | \\ m_3 \end{array} = \begin{array}{c} n_1 \quad n_2 \quad n_3 \\ j_1 \quad j_2 \quad j_3 \\ \hline + \\ j_1 \quad j_2 \quad j_3 \\ m_1 \quad m_2 \quad m_3 \end{array}. \quad (2.35)$$

In SFMs, one usually needs also to evaluate the integration over the product of irreducible representations of g_e and its inverse $g_e^{-1} = g_{e^{-1}}$. This can be accomplished by combining Eq. (2.32) with Eq. (2.29). For example, the integration over the product of $n - 1$ irreducible representations of g_e and one representation of g_e^{-1} is given graphically by

$$\begin{aligned} & \int dg_e \begin{array}{c} n_1 \\ | \\ e \leftarrow j_1 \\ | \\ m_1 \end{array} \begin{array}{c} n_2 \\ | \\ e \leftarrow j_2 \\ | \\ m_2 \end{array} \cdots \begin{array}{c} n_{n-1} \\ | \\ e^{-1} \leftarrow j_{n-1} \\ | \\ m_{n-1} \end{array} \begin{array}{c} n_n \\ | \\ e \leftarrow j_n \\ | \\ m_n \end{array} \\ &= \int dg_e \begin{array}{c} n_1 \\ | \\ e \leftarrow j_1 \\ | \\ m_1 \end{array} \begin{array}{c} n_2 \\ | \\ e \leftarrow j_2 \\ | \\ m_2 \end{array} \begin{array}{c} n_{n-1} \\ | \\ e \leftarrow j_{n-1} \\ | \\ m_{n-1} \end{array} \begin{array}{c} n_n \\ | \\ e \leftarrow j_n \\ | \\ m_n \end{array} \\ &= \sum_{\{a_2, \dots, a_{n-2}\}} \prod_{i=2}^{n-2} d_{a_i} \begin{array}{c} n_1 \quad n_2 \quad \cdots \quad n_{n-1} \quad n_n \\ j_1 \quad j_2 \quad \cdots \quad j_{n-1} \quad j_n \\ \hline - \quad a_2 \quad \cdots \quad a_{n-2} \quad + \\ + \quad a_2 \quad \cdots \quad a_{n-2} \quad - \\ j_1 \quad j_2 \quad \cdots \quad j_{n-1} \quad j_n \\ m_1 \quad m_2 \quad \cdots \quad m_{n-1} \quad m_n \end{array}. \quad (2.36) \end{aligned}$$

Thus the integration leads to a summation of products of (normalized) two intertwiners i_{v_1} and i_{v_2} associated to two endpoints v_1 and v_2 of e . Each of the intertwiners has an arrow on the external line associated to g_e^{-1} while the other external lines have no arrows. By the transformation rules (2.17)-(2.20), the above result can be transformed to an equivalent form such that each external lines associated to g_e has an arrow while the external line associated to g_e^{-1} has no arrow. In the case that the orientations of edges are irrelevant to the question considered, the corresponding integration can be roughly expressed as

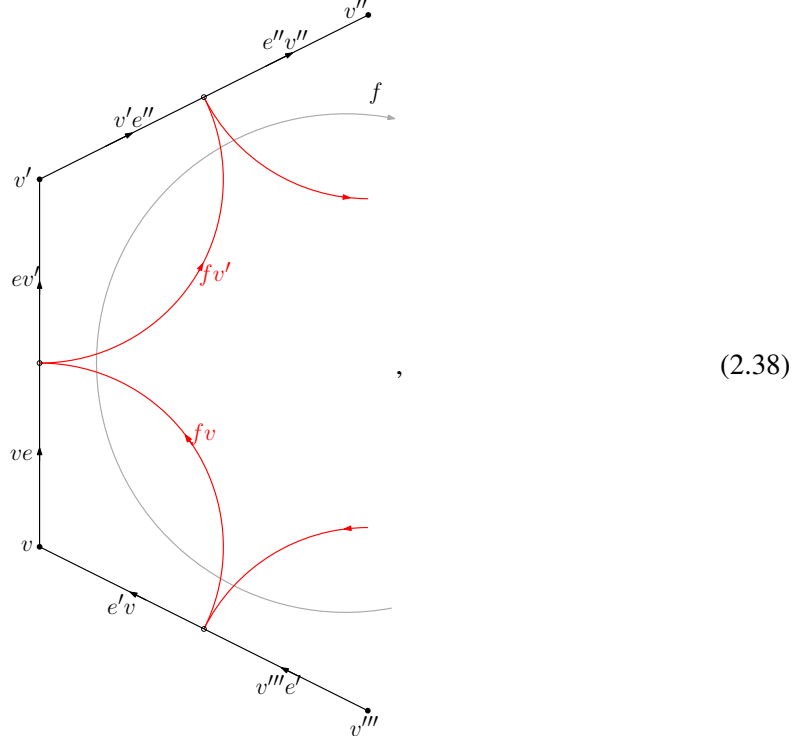
$$\int dg_e \begin{array}{c} n_1 \\ | \\ e \leftarrow j_1 \\ | \\ m_1 \end{array} \begin{array}{c} n_2 \\ | \\ e \leftarrow j_2 \\ | \\ m_2 \end{array} \cdots \begin{array}{c} n_{n-1} \\ | \\ e \leftarrow j_{n-1} \\ | \\ m_{n-1} \end{array} \begin{array}{c} n_n \\ | \\ e \leftarrow j_n \\ | \\ m_n \end{array} = \begin{array}{c} n_1 \quad n_2 \quad \cdots \quad n_{n-1} \quad n_n \\ j_1 \quad j_2 \quad \cdots \quad j_{n-1} \quad j_n \\ \hline + \quad \cdots \quad + \\ j_1 \quad j_2 \quad \cdots \quad j_{n-1} \quad j_n \\ m_1 \quad m_2 \quad \cdots \quad m_{n-1} \quad m_n \end{array}. \quad (2.37)$$

We will adopt the rough formula (2.37) to derive the partition function in the following two subsections. Certain explicit formula with orientations of edges similar to (2.36) will be considered in Sec. 4.

2.2 The partition function in non-boundary cases

Let us consider the underlying dual 2-cell Δ^* without boundary, and derive the partition function on Δ^* from Eq. (2.2) by the graphical calculus presented in the previous subsection. We single out a part

of an oriented face f of Δ^* as



where the orientations of boundary edges $e \in \partial f$, represented by the arrows, are induced by that of f . Here the (internal) vertices (endpoints) v of the (internal) edges e were denoted by the solid points, while the midpoints of e were represented by hollow circles, by which each edge e is broke into two segments ve and ev' with orientations agreeing with that of e , and the oriented red curves lying in f represents the edges fv of the vertex-boundary graphs γ_v based at v . In non-boundary cases, the partition function (2.2) reduces to

$$\begin{aligned}
\mathcal{Z}^{\text{BF}}(\Delta^*) &= \int dg_{fv}^+ \prod_{f \in \Delta^*} \sum_{j_f^+} d_{j_f^+} \text{Tr}_{j_f^+} \left(\prod_{v \in \partial f} g_{fv}^+ \right) \prod_{fv} \int dg_{ve}^+ \sum_{j_{fv-1}^+} d_{j_{fv-1}^+} \text{Tr}_{j_{fv-1}^+} (g_{e'v}^+ g_{ve}^+ g_{fv-1}^+) \\
&\quad \times \int dg_{fv}^- \prod_{f \in \Delta^*} \sum_{j_f^-} d_{j_f^-} \text{Tr}_{j_f^-} \left(\prod_{v \in \partial f} g_{fv}^- \right) \prod_{fv} \int dg_{ve}^- \sum_{j_{fv-1}^-} d_{j_{fv-1}^-} \text{Tr}_{j_{fv-1}^-} (g_{e'v}^- g_{ve}^- g_{fv-1}^-) \\
&\equiv \int dg_{fv}^+ dg_{fv}^- \prod_{f \in \Delta^*} A_f^{\text{BF}}(\{g_{fv}^+, g_{fv}^-\}).
\end{aligned} \tag{2.39}$$

To derive a partition function $Z^{\text{SFM}}(\Delta^*)$ from (2.39), one can follow the three steps introduced below Eq. (2.3).

First, we need to perform the $dg_{ve}^+ dg_{ve}^-$ integration in the first equality in Eq. (2.39) to obtain the expression of A_f^{BF} . Notice that a segment ve bounded by n faces contributes the partition function (2.39) n pairs (g_{ve}^+, g_{ve}^-) of matrix elements to be integrated out. To preform the integration, we firstly

transform the algebraic formula (2.39) into its graphical formula. Thanks to the graphical calculus presented in Eq. (2.37), the $dg_{ve}^+ dg_{ve}^-$ integration can be straightforwardly evaluated to yield

$$A_f^{\text{BF}}(\{g_{fv}^+, g_{fv}^-\}) = \text{Diagram} \quad , \quad (2.40)$$

The diagram illustrates the graphical evaluation of the BF action. It consists of three vertically stacked terms, each representing a different configuration of holonomies and intertwiners. The central vertical line represents an edge e with endpoints v and v' . Intertwiners i_e^{\pm} are shown at the vertices and midpoints. Curved lines represent holonomies: red for g_{fv}^+ and dark green for g_{fv}^- . Labels include j_f^{\pm} , $f v$, $f v^{-1}$, and summations over $d_{j_f^{\pm}}$.

where the oriented red and dark green curved lines denote respectively the matrix elements of g^+ attached to edges fv of γ_v and their inverses fv^{-1} , while those of g^- are omitted for simplicity. It should be noted that the pairs (i_e^+, i_e^-) of intertwiners, as well as (i_e^-, i_e^-) , associated to the endpoint pair (v, v') have certain arrows (the “metrics”) with uniform orientations on their external lines, while the intertwiners associated to the midpoints of e have no arrows on their external lines. The origin of these arrows is the following. For a given internal edge e bounded by faces $f \in \partial e$, each f induces an orientation on e and contributes a holonomy with representation j_f . If the induced orientations on e from different faces are not the same, the induced holonomies with spins j_f will involve g_e as well as $g_{e^{-1}}$ associated to e . However, the representations of $g_{e^{-1}}$ can be uniformly transformed to those of g_e by adding two arrows to the graphical representation of the corresponding holonomy associated to the endpoints v and v' of e by the graphical rule (2.29).

Second, we need to impose the simplicity constraint. In the Euclidean EPRL model as well as its generalized model, the simplicity constraint was firstly expressed as the corresponding linear formulation and then imposed at quantum level by the master-constraint criterion [38, 48] or the Gupta-Bleuler criterion [40]. The result restricts the relation between j^{\pm} and their coupling j associated to

f , depending on the values of the Immirzi parameter β , as [10, 38, 42, 43]

$$\begin{cases} j^\pm = (1 \pm \beta)j/2, & \text{for } \beta < 1 \\ j^\pm = (\beta \pm 1)j/2, & \text{for } \beta > 1 \end{cases}, \quad (2.41)$$

and thus

$$\begin{cases} j = j^+ + j^-, & \text{for } \beta < 1 \\ j = j^+ - j^-, & \text{for } \beta > 1 \end{cases}. \quad (2.42)$$

For the turning point $\beta = 1$, one has

$$j^+ = j, \quad j^- = 0. \quad (2.43)$$

Hence the quantum simplicity constraint can be imposed as a projection by the so-called \mathcal{Y} -map

$$\mathcal{Y} : \mathcal{H}_{j^+} \otimes \mathcal{H}_{j^-} = \oplus_{j'=|j^+-j^-|}^{j^++j^-} \mathcal{H}_{j'} \rightarrow \mathcal{H}_j. \quad (2.44)$$

It naturally induces a Y -map with actions on intertwiners and holonomies graphically as

$$Y \begin{array}{c} n^+ \\ | \\ j^+ \\ | \\ m^+ \end{array} \begin{array}{c} n^- \\ | \\ j^- \\ | \\ m^- \end{array} = Y \sum_{j'=|j^+-j^-|}^{j^++j^-} d_{j'} \begin{array}{c} n^+ \quad n^- \\ \diagdown \quad \diagup \\ j^+ \quad j^- \\ | \\ j' \\ | \\ j^+ \quad j^- \\ \diagup \quad \diagdown \\ m^+ \quad m^- \end{array} := d_j \begin{array}{c} n^+ \quad n^- \\ \diagdown \quad \diagup \\ j^+ \quad j^- \\ | \\ j \\ | \\ j^+ \quad j^- \\ \diagup \quad \diagdown \\ m^+ \quad m^- \end{array}, \quad (2.45)$$

and

$$Y \begin{array}{c} m^+ \xrightarrow{j^+} n^+ \\ m^- \xrightarrow{j^-} n^- \end{array} = Y \sum_{j'=|j^+-j^-|}^{j^++j^-} d_{j'} \begin{array}{c} m^+ \quad j^+ \\ \diagdown \quad \diagup \\ m^- \quad j^- \end{array} \xrightarrow{j'} \begin{array}{c} j^+ \quad n^+ \\ \diagdown \quad \diagup \\ j^- \quad n^- \end{array} := d_j \begin{array}{c} m^+ \quad j^+ \\ \diagdown \quad \diagup \\ m^- \quad j^- \end{array} \xrightarrow{j} \begin{array}{c} j^+ \quad n^+ \\ \diagdown \quad \diagup \\ j^- \quad n^- \end{array}. \quad (2.46)$$

By imposing the Y -map (2.45) on the intertwiners associated to the vertices of γ_v , the partition function $\mathcal{Z}^{\text{BF}}(\Delta^*)$ in Eq. (2.39) can be promoted to the (Euclidean) generalized EPRL partition function

$$\mathcal{Z}^{\text{EPRL}}(\Delta^*) := \int dg_{f_v}^+ dg_{f_v}^- \prod_{f \in \Delta^*} A_f^{\text{EPRL}}(\{g_{f_v}^+, g_{f_v}^-\}) \quad (2.47)$$

with

$$A_f^{\text{EPRL}}(\{g_{f_v}^+, g_{f_v}^-\}) := Y \cdot A_f^{\text{BF}}(\{g_{f_v}^+, g_{f_v}^-\})$$

$$= \text{[Diagrammatic Equation (2.48)]} , \quad (2.48)$$

where Eqs. (2.45) and (2.24) was used in the second and third steps respectively.

Third, we need to perform the integration over the group elements g_{fv}^\pm associated to each vertex v . In the current case, Eq. (2.34) becomes

$$\int dg_{fv}^+ \text{ [Diagrammatic Expression] } = \frac{\delta_{j_{fv}^{-1}, j_f^+}}{d_{j_{fv}^{-1}}} \cdot \text{[Diagrammatic Expression]} . \quad (2.49)$$

By the integration, Eq. (2.47) reduces to

$$\mathcal{Z}^{\text{EPRL}}(\Delta^*) = \prod_{f \in \Delta^*} \left(\text{Diagram 1} \right) = \prod_{f \in \Delta^*} \left(\text{Diagram 2} \right), \quad (2.50)$$

The diagram on the left shows a vertex v with four incident edges e . Each edge e is associated with an intertwiner i_e^+ and i_e^- . The vertex v is associated with a vertex amplitude A_v . The edges e are also associated with fusion coefficients $d_{j_f^+} d_{j_f^-}$. The diagram on the right shows a similar vertex v with four incident edges e , but the edges e are now associated with intertwiners i_e^+ and i_e^- and fusion coefficients $d_{j_f^+} d_{j_f^-}$. The vertex v is associated with a vertex amplitude A_v . The edges e are also associated with fusion coefficients $d_{j_f^+} d_{j_f^-}$.

where in the second step we used

$$\left(\text{Diagram 3} \right) = \left(\text{Diagram 4} \right) = \delta_{i_e, i'_e}, \quad (2.51)$$

The diagram on the left shows a vertex v with four incident edges e . Each edge e is associated with an intertwiner i_e^+ and i_e^- . The vertex v is associated with a vertex amplitude A_v . The edges e are also associated with fusion coefficients $d_{j_f^+} d_{j_f^-}$. The diagram on the right shows a similar vertex v with four incident edges e , but the edges e are now associated with intertwiners i_e^+ and i_e^- and fusion coefficients $d_{j_f^+} d_{j_f^-}$. The vertex v is associated with a vertex amplitude A_v . The edges e are also associated with fusion coefficients $d_{j_f^+} d_{j_f^-}$.

in the light of Eq. (2.14). The resulting partition function $\mathcal{Z}^{\text{EPRL}}(\Delta^*)$ in Eq. (2.50) assigns to each internal vertex v a contraction of intertwiners $i_e^+ \otimes i_e^-$ associated to edges $e \in \partial v$, as a vertex amplitude A_v , to each internal edge e a fusion coefficient

$$f_{i_e^+ i_e^-}^{i_e} \equiv \left(\text{Diagram 5} \right), \quad (2.52)$$

The diagram on the left shows a vertex v with four incident edges e . Each edge e is associated with an intertwiner i_e^+ and i_e^- . The vertex v is associated with a vertex amplitude A_v . The edges e are also associated with fusion coefficients $d_{j_f^+} d_{j_f^-}$.

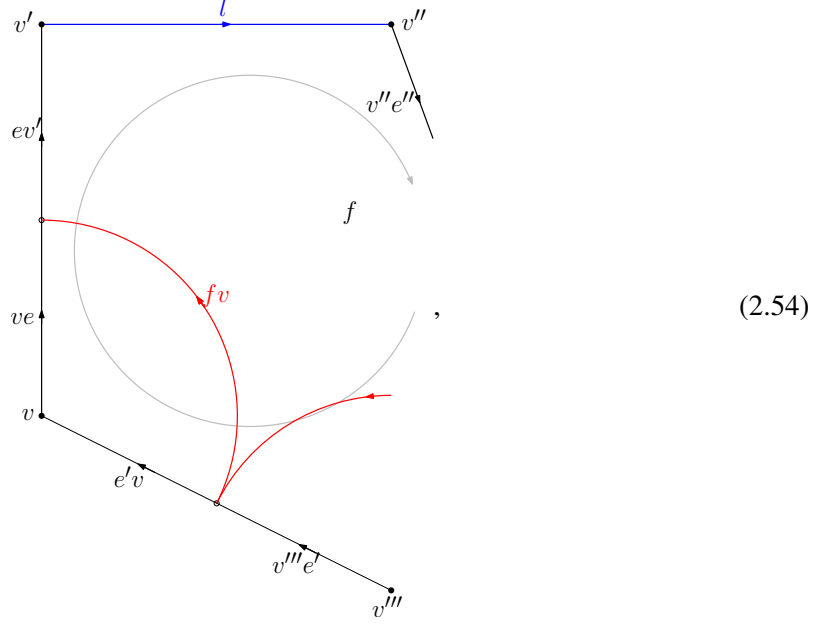
as an edge amplitude A_e , and to each face f a factor $d_{j_f^+} d_{j_f^-}$ as a face amplitude A_f . The graphical formula of $\mathcal{Z}^{\text{EPRL}}(\Delta^*)$ presented in Eq. (2.50) can be uniquely transformed into its algebraic formula

$$\mathcal{Z}^{\text{EPRL}}(\Delta^*) = \sum_{j_f^+, j_f^-} \prod_{f \in \Delta^*} d_{j_f^+} d_{j_f^-} \prod_{v \in \Delta^*} \sum_{i_e^+, i_e^-, i_e} \text{Tr}_v \left[\bigotimes_{e \in \partial v} (i_e^+ \otimes i_e^-) \right] \prod_{e \in \partial v} f_{i_e^+ i_e^-}^{i_e}, \quad (2.53)$$

which coincides with the one appeared in Refs. [32, 43].

2.3 The partition function in cases with boundaries

Now let us consider the underlying dual 2-cell Δ^* with a boundary. We single out a part of Δ^* consisting of an oriented face f bounded by a global boundary edge l as



where the red curves denotes again the edges fv of the vertex boundary graph γ_v lying in f based at internal vertices v , and the blue curve represents the global boundary edge l . The derivation of the resulting partition function is quite similar to that in the non-boundary cases. Now Eq. (2.2) can be denoted by

$$\mathcal{Z}^{\text{BF}}(\Delta^*) = \int dg_{fv}^+ dg_{fv}^- \prod_{f \in \Delta^*} A_f^{\text{BF}}(\{g_{fv}^+, g_{fv}^-, g_l^+, g_l^-\}). \quad (2.55)$$

Integrating over the group elements g_{ve}^\pm associated to the internal edges of Δ^* yields

Here the notations are the same as those for the non-boundary case.

Imposing the Y -map on the intertwiners associated to the vertices of γ_v and on the holonomies associated to edges l on the boundaries by Eqs. (2.45) and (2.46), the partition function $\mathcal{Z}^{\text{BF}}(\Delta^*)$ in Eq. (2.55) can be promoted to the (Euclidean) generalized EPRL partition function

$$\mathcal{Z}^{\text{EPRL}}(\Delta^*) := \int \mathrm{d}g_{fv}^+ \mathrm{d}g_{fv}^- \prod_{f \in \Delta^*} A_f^{\text{EPRL}}(\{g_{fv}^+, g_{fv}^-, g_l\}) \quad (2.57)$$

with

$$A_f^{\text{EPRL}}(\{g_{fv}^+, g_{fv}^-, g_l\}) := Y \cdot A_f^{\text{BF}}(\{g_{fv}^+, g_{fv}^-, g_l^+, g_l^-\})$$

(2.58)

– 19 –

Using Eq. (2.49), the integration over $dg_{f_v}^+ dg_{f_v}^+$ in Eq. (2.57) yields

$$\mathcal{Z}^{\text{EPRL}}(\Delta^*) = \prod_{f \in \Delta^*} \left[\text{Diagram} \right] = \prod_{f \in \Delta^*} \left[\text{Simplified Diagram} \right], \quad (2.59)$$

where in the second step we used

$$\left[\text{Diagram} \right] = \left[\text{Simplified Diagram} \right] = \delta_{j_f, j_l} \delta_{i_e', i_e}, \quad (2.60)$$

in the light of Eqs. (2.24), (2.14), (2.19) and (2.15). The resulting partition function $\mathcal{Z}^{\text{EPRL}}(\Delta^*)$ expressed in the graphical formula (2.59) can be uniquely transformed into the algebraic formula

$$\mathcal{Z}^{\text{EPRL}}(\Delta^*) = \sum_{j_f^+, j_f^-} \prod_{f \in \Delta^*} d_{j_f^+} d_{j_f^-} \prod_{v \in \Delta^*} \sum_{i_e^+, i_e^-, i_e'} \text{Tr}_v \left[\bigotimes_{e \in \partial v} (i_e^+ \otimes i_e^-) \right] \prod_{e \in \partial v} f_{i_e^+ i_e^-}^{i_e'} \sum_{j_l, i_v} \left(\prod_{l \in \partial \Delta^*} \frac{1}{\sqrt{d_{j_l}}} \right) T_{\partial \Delta^*, \vec{j}_l, \vec{i}_v}(\{g_l\}), \quad (2.61)$$

where $\vec{i}_v := i_e'$ denotes the set of the normalized gauge-invariant intertwiners associated to the boundary vertices $v \in \partial \Delta^*$, and $T_{\partial \Delta^*, \vec{j}_l, \vec{i}_v}(\{g_l\})$ denotes the normalized gauge-invariant spin network states on $\partial \Delta^*$. Given the “in” and “out” kinematical states ψ_s and $\psi_{s'}$ on $\partial \Delta^*$, the transition amplitude between them is defined by

$$\sum_{\partial \Delta^* = \psi_s \cup \psi_{s'}} \langle \psi_{s'} | \mathcal{Z}^{\text{EPRL}}(\Delta^*) | \psi_s \rangle := \sum_{\partial \Delta^* = \psi_s \cup \psi_{s'}} \sum_{j_f^+, j_f^-} \prod_{f \in \Delta^*} d_{j_f^+} d_{j_f^-} \prod_{v \in \Delta^*} \sum_{i_e^+, i_e^-, i_e'} \text{Tr}_v \left[\bigotimes_{e \in \partial v} (i_e^+ \otimes i_e^-) \right] \prod_{e \in \partial v} f_{i_e^+ i_e^-}^{i_e'}$$

$$\times \left(\prod_{l \in \partial \Delta^*} \frac{1}{\sqrt{d_{jl}}} \right), \quad (2.62)$$

where the summation $\sum_{\partial \Delta^* = \psi_s \cup \psi_{s'}}$ is taken over all possible Δ^* whose boundary states consist of ψ_s and $\psi_{s'}$.

3 Matrix elements of a Hamiltonian constraint operator

In the Hamiltonian formulation of GR, the Hamiltonian constraint for pure gravity in the Ashtekar-Barbero variables smeared with an arbitrary function N on the spatial manifold Σ reads [2, 13]

$$\mathcal{H}_{\text{grav}}(N) = \int_{\Sigma} d^3x \frac{N \tilde{E}_i^a \tilde{E}_j^b}{2\kappa \sqrt{\det(q)}} \left[\epsilon^{ij}{}_k F_{ab}^k - 2(-\zeta + \beta^2) K_{[a}^i K_{b]}^j \right], \quad (3.1)$$

where $\det(q)$ is the determinant of the spatial metric q_{ab} on Σ , ζ denotes the spacetime signature such that $\zeta = -1$ and $\zeta = +1$ represent for the Lorentzian and Euclidean cases respectively, F_{ab}^i is the curvature of connection A_a^i , and K_a^i represents the extrinsic curvature of Σ . In the Euclidean case of $\zeta = +1$, by taking the Immirzi parameter $\beta = 1$, Eq. (3.1) is reduced to the so-called Euclidean term

$$\mathcal{H}_{\text{grav}}^{\text{E}}(N) := \int_{\Sigma} d^3x N \frac{\tilde{E}_i^a \tilde{E}_j^b}{2\kappa \sqrt{\det(q)}} \epsilon^{ij}{}_k F_{ab}^k. \quad (3.2)$$

Different candidate Hamiltonian constraint operators corresponding to $\mathcal{H}_{\text{grav}}^{\text{E}}(N)$ have been proposed for canonical LQG. Here we consider the Hamiltonian constraint operator $\hat{H}^{\text{E}}(N)$ defined in [26], which is well defined in certain partially diffeomorphism invariant Hilbert space \mathcal{H}_{np4} and can be promoted as a symmetric operator. To simplify the discussion, we choose a corresponding regulated operator $\hat{H}_{\delta}^{\text{E}}(N)$ in the kinematical Hilbert space \mathcal{H}_{kin} in following calculations. Since the operators $\hat{H}_{\delta}^{\text{E}}(N)$ for different δ belong to the same diffeomorphism equivalent class [26], all our calculations are also valid for the operator $\hat{H}^{\text{E}}(N)$ in \mathcal{H}_{np4} . By a special operator ordering, the action of $\hat{H}_{\delta}^{\text{E}}(N)$ on a cylindrical function f_{γ} over a graph γ with edges outgoing from its vertices v reads

$$\hat{H}_{\delta}^{\text{E}}(N) \cdot f_{\gamma} = -\frac{3(\beta \ell_{\text{p}}^2)^2}{\kappa \chi(m)^2} \sum_{v \in V(\gamma)} N_v \hat{H}_v^{\text{E}} \cdot f_{\gamma}, \quad (3.3)$$

where

$$\chi(x) := \sqrt{x(x+1)(2x+1)}, \quad (3.4)$$

and

$$\hat{H}_v^{\text{E}} := \sum_{e_i \cap e_j = v} \hat{H}_{v, e_i, e_j}^{\text{E}} \quad (3.5)$$

with

$$\hat{H}_{v, e_i, e_j}^{\text{E}} := \epsilon_{klm} \text{Tr}_m(\tau_k g_{\alpha_{ij}}) J_i^l J_j^m \widehat{V^{-1}}_v$$

$$\begin{aligned}
&= -i\epsilon_{\mu\nu\rho}\text{Tr}_m(\tau_\mu g_{\alpha_{ij}})J_i^\nu J_j^\rho \widehat{V^{-1}}_v \\
&= -i\epsilon_{\mu\nu\rho}[\pi_m(\tau_\mu)]^A_B[\pi_m(g_{\alpha_{ij}})]^B_A J_i^\nu J_j^\rho \widehat{V^{-1}}_v.
\end{aligned} \tag{3.6}$$

Here the trace Tr_m is taken in the irreducible representation π_m of $SU(2)$, $g_{\alpha_{ij}}$ represents the holonomies along loops $\alpha_{ij} = s_i \circ a_{ij} \circ s_j^{-1}$ based at the vertices v consisting of two segments s_i and s_j of e_i and e_j and the arc a_{ij} connecting two endpoints of s_i and s_j , the orientation of α_{ij} has been specially chosen such that it agrees with the one induced by Σ , $J_i^l \equiv J_{e_i}^l$ is the self-adjoint right-invariant vector field on a copy of $SU(2)$ associated to e_i , $\widehat{V^{-1}}_v$ denotes the inverse volume operator

$$\widehat{V^{-1}} := \lim_{\lambda \rightarrow 0} \frac{\hat{V}}{\hat{V}^2 + (\lambda \ell_p^3)^2} \tag{3.7}$$

acting at vertices v , $\epsilon_{\mu\nu\rho}$ ($\mu, \nu, \rho = 0, +1, -1$) is the Levi-Civita symbol defined by $\epsilon_{-1\ 0\ +1} = 1$, and τ_μ ($\mu = 0, \pm 1$) is the spherical tensor, which is related to the basis $\tau_i := -i\sigma_i/2$ ($i = 1, 2, 3$) of $su(2)$ with σ_i being the Pauli matrices by

$$\tau_0 := \tau_3, \quad \tau_\pm := \mp \frac{1}{\sqrt{2}}(\tau_1 \pm i\tau_2). \tag{3.8}$$

Intuitively, the operator \hat{H}_v^E acts on γ by attaching an arc a_{ij} to each pair (e_i, e_j) of edges such that the resulting loop $\alpha_{ij} = e_i \circ a_{ij} \circ e_j^{-1}$ has a positive orientation. Notice that the operator $\widehat{V^{-1}}_v$ in Eq. (3.7) vanishes at a gauge-invariant vertex v with valence less than four by the property of the volume operator \hat{V} [20]. Consider a simply graph γ with a non-coplanar vertex v and four edges e_1, \dots, e_4 starting from v . To specify a spin network state to γ , one needs to specify spins j_1, \dots, j_4 to its edges e_1, \dots, e_4 and a gauge-invariant intertwiner to v . To specify the intertwiner, one needs to choose a coupling scheme for j_1, \dots, j_4 and an intermediate coupling spin. Different coupling schemes are related by the $6j$ -symbol. For example, the following formula relates the two different coupling schemes for the intertwiners associated to v [44, 45]

$$\begin{array}{c} m_1 \\ j_1 \\ + \\ j_3 \\ m_3 \end{array} \xrightarrow{j_5} \begin{array}{c} j_4 \\ + \\ j_2 \\ m_2 \end{array} \xrightarrow{j_6} \begin{array}{c} m_3 \\ j_3 \\ + \\ j_2 \\ m_2 \end{array} \xrightarrow{j_6} \begin{array}{c} j_1 \\ + \\ j_4 \\ m_4 \end{array} = \sum_{j_6} d_{j_6} (-1)^{j_1-j_2+j_3+j_4} \begin{Bmatrix} j_1 & j_4 & j_6 \\ j_2 & j_3 & j_5 \end{Bmatrix} \begin{array}{c} m_3 \\ j_3 \\ + \\ j_2 \\ m_2 \end{array} \xrightarrow{j_6} \begin{array}{c} j_1 \\ + \\ j_4 \\ m_4 \end{array}. \tag{3.9}$$

Given a gauge-invariant spin network state ψ_s on γ with a specified intertwiner at v , the action of \hat{H}_v^E on ψ_s is given by

$$\begin{aligned}
\hat{H}_v^E \cdot \psi_s &= \sum_{e_i \cap e_j = v} \hat{H}_{v, e_i, e_j}^E \cdot \psi_s \\
&= \sum_{e_i \cap e_j = v} \hat{H}_{v, e_i, e_j}^E \cdot \sum_i f_s^i \sqrt{d_{j_i} d_{j_j} d_{j_k} d_{j_l} d_i} \begin{array}{c} j_l \\ e_l \\ + \\ j_i \\ e_i \end{array} \xrightarrow{i} \begin{array}{c} j_k \\ e_k \\ + \\ j_j \\ e_j \end{array} \\
&= \sum_i f_s^i \sum_{e_i \cap e_j = v} \hat{H}_{v, e_i, e_j}^E \cdot \sqrt{d_{j_i} d_{j_j} d_{j_k} d_{j_l} d_i} \begin{array}{c} j_l \\ e_l \\ + \\ j_i \\ e_i \end{array} \xrightarrow{i} \begin{array}{c} j_k \\ e_k \\ + \\ j_j \\ e_j \end{array}, \tag{3.10}
\end{aligned}$$

where f_s^i are the expanding factors involving $6j$ -symbols. Hence, one only needs to evaluate the action of \hat{H}_{v,e_i,e_j}^E on the normalized spin network state

$$\psi_i = \sqrt{d_{j_i} d_{j_j} d_{j_k} d_{j_l} d_i} \begin{array}{c} \text{Diagram: A central vertex } i \text{ with four edges. Top-left edge } j_l \text{ with label } e_l \text{ and a blue slash. Bottom-left edge } j_i \text{ with label } e_i \text{ and a blue slash. Top-right edge } j_k \text{ with label } e_k \text{ and a blue slash. Bottom-right edge } j_j \text{ with label } e_j \text{ and a blue slash. All edges are directed towards the central vertex } i. \end{array} \quad (3.11)$$

Notice that the Levi-Civita symbol $\epsilon_{\mu\nu\rho}$ is related to the $3j$ -symbols by [44]

$$\epsilon_{\mu\nu\rho} = \chi(1) \begin{pmatrix} 1 & 1 & 1 \\ \mu & \nu & \rho \end{pmatrix} = \chi(1) \begin{array}{c} \nu \quad \rho \\ \diagdown \quad \diagup \\ 1 \\ \diagup \quad \diagdown \\ \mu \end{array}, \quad (3.12)$$

the spherical tensors τ_μ can be represented by [44]

$$[\pi_j(\tau_\mu)]^A_B = i\chi(j) \begin{array}{c} \mu \\ | \\ 1 \\ \hline A \xrightarrow{j} + \xrightarrow{j} B \end{array} = i\chi(j) \begin{array}{c} \mu \\ | \\ 1 \\ \hline B \xrightarrow{j} - \xrightarrow{j} A \end{array}, \quad (3.13)$$

and the action of J_i^μ on a spin network state is determined by its action on the corresponding intertwiner as [44]

$$J_i^\mu \prod_{i=2}^{n-2} \sqrt{d_{a_i}} \begin{array}{c} m_1 \quad m_2 \quad \dots \quad m_i \quad \dots \quad m_{n-1} \quad m_n \\ | \quad | \quad \dots \quad | \quad \dots \quad | \quad | \\ j_1 \quad j_2 \quad \dots \quad j_i \quad \dots \quad j_{n-1} \quad j_n \\ \hline -a_2 \quad \dots \quad a_{n-2} \end{array} = \chi(j_i) \prod_{i=2}^{n-2} \sqrt{d_{a_i}} \begin{array}{c} m_1 \quad m_2 \quad \dots \quad m_i \quad \dots \quad m_{n-1} \quad m_n \\ | \quad | \quad \dots \quad | \quad \dots \quad | \quad | \\ j_1 \quad j_2 \quad \dots \quad j_i \quad \dots \quad j_{n-1} \quad j_n \\ \hline -a_2 \quad \dots \quad a_{n-2} \end{array}. \quad (3.14)$$

Thus, the action of \hat{H}_{v,e_i,e_j}^E on ψ_i can be calculated as

$$\begin{aligned} \hat{H}_{v,e_i,e_j}^E \sqrt{d_i} \begin{array}{c} \text{Diagram: A central vertex } i \text{ with four edges. Top-left edge } j_l \text{ with label } e_l \text{ and a blue slash. Bottom-left edge } j_i \text{ with label } e_i \text{ and a blue slash. Top-right edge } j_k \text{ with label } e_k \text{ and a blue slash. Bottom-right edge } j_j \text{ with label } e_j \text{ and a blue slash. All edges are directed towards the central vertex } i. \end{array} &= -i\epsilon_{\mu\nu\rho} [\pi_m(\tau_\mu)]^A_B [\pi_m(g_{\alpha_{ij}})]^B_A J_i^\nu J_j^\rho \sum_k \left(\widehat{V^{-1}_v} \right)_i^k \sqrt{d_k} \begin{array}{c} \text{Diagram: A central vertex } k \text{ with four edges. Top-left edge } j_l \text{ with label } e_l \text{ and a blue slash. Bottom-left edge } j_i \text{ with label } e_i \text{ and a blue slash. Top-right edge } j_k \text{ with label } e_k \text{ and a blue slash. Bottom-right edge } j_j \text{ with label } e_j \text{ and a blue slash. All edges are directed towards the central vertex } k. \end{array} \\ &= \chi(1) \chi(m) \chi(j_i) \chi(j_j) \sum_k \left(\widehat{V^{-1}_v} \right)_i^k \sqrt{d_k} \sum_{a,b} d_a d_b \begin{array}{c} \text{Diagram: A complex diagram showing a central vertex } k \text{ with four edges. Top-left edge } j_l \text{ with label } e_l \text{ and a blue slash. Bottom-left edge } j_i \text{ with label } e_i \text{ and a blue slash. Top-right edge } j_k \text{ with label } e_k \text{ and a blue slash. Bottom-right edge } j_j \text{ with label } e_j \text{ and a blue slash. All edges are directed towards the central vertex } k. \text{ Below this, there is a diagram with two vertices } i \text{ and } j. \text{ Vertex } i \text{ has edges } j_i^1 \text{ (top) and } j_i^2 \text{ (bottom). Vertex } j \text{ has edges } j_j^1 \text{ (top) and } j_j^2 \text{ (bottom). There are horizontal edges } a \text{ and } b \text{ between } i \text{ and } j. \text{ There are also curved edges } m \text{ between } i \text{ and } j. \end{array} \\ &= \chi(1) \chi(m) \chi(j_i) \chi(j_j) \sum_k \left(\widehat{V^{-1}_v} \right)_i^k \sqrt{d_k} \sum_{a,b} d_a d_b \end{aligned}$$

$$\begin{aligned}
& \times \sum_c d_c (-1)^{b+c+j_j-1} \begin{Bmatrix} c & j_i & a \\ j_i & m & 1 \end{Bmatrix} \begin{Bmatrix} c & j_j & b \\ j_j & m & 1 \end{Bmatrix} \begin{Bmatrix} c & m & 1 \\ 1 & 1 & m \end{Bmatrix} \\
& \times \sum_t d_t (-1)^{j_l-j_i-k} (-1)^{t+b-j_k} \begin{Bmatrix} t & j_l & a \\ j_i & c & k \end{Bmatrix} \begin{Bmatrix} t & j_k & b \\ j_j & c & k \end{Bmatrix} \\
& \times \text{Diagram} \quad , \tag{3.15}
\end{aligned}$$

where $\left(\widehat{V^{-1}}\right)_i^k \equiv \langle i_v^k | \widehat{V^{-1}}_v | i_v^i \rangle$ denote the matrix elements of $\widehat{V^{-1}}_v$ between intertwiners i_v^i and i_v^k associated to v and labeled by the intermediate angular momenta i and k , and in the last step we used

$$\begin{aligned}
& \text{Diagram} = \sum_{c,d} d_c d_d \text{Diagram} \\
& = \sum_c d_c (-1)^{b+c+j_j-1} \begin{Bmatrix} c & j_i & a \\ j_i & m & 1 \end{Bmatrix} \begin{Bmatrix} c & j_j & b \\ j_j & m & 1 \end{Bmatrix} \begin{Bmatrix} c & m & 1 \\ 1 & 1 & m \end{Bmatrix} \text{Diagram} \\
& = \sum_c d_c (-1)^{b+c+j_j-1} \begin{Bmatrix} c & j_i & a \\ j_i & m & 1 \end{Bmatrix} \begin{Bmatrix} c & j_j & b \\ j_j & m & 1 \end{Bmatrix} \begin{Bmatrix} c & m & 1 \\ 1 & 1 & m \end{Bmatrix} \sum_t d_t \text{Diagram} \\
& = \sum_c d_c (-1)^{b+c+j_j-1} \begin{Bmatrix} c & j_i & a \\ j_i & m & 1 \end{Bmatrix} \begin{Bmatrix} c & j_j & b \\ j_j & m & 1 \end{Bmatrix} \begin{Bmatrix} c & m & 1 \\ 1 & 1 & m \end{Bmatrix} \\
& \quad \times \sum_t d_t (-1)^{j_l-j_i-k} (-1)^{t+b-j_k} \begin{Bmatrix} t & j_l & a \\ j_i & c & k \end{Bmatrix} \begin{Bmatrix} t & j_k & b \\ j_j & c & k \end{Bmatrix} \text{Diagram} . \tag{3.16}
\end{aligned}$$

Note that to derive Eq. (3.16), we used Eqs. (2.13), (2.17) and (2.19) in the first step, the identities

$$\begin{aligned}
& \text{Diagram} = (-1)^{m+1+c} (-1)^{2j_i+1} (-1)^{2j_i} (-1)^{m+a+j_i} \text{Diagram} = (-1)^{2m+j_i+a+c} \begin{Bmatrix} c & j_i & a \\ j_i & m & 1 \end{Bmatrix} \text{Diagram} \\
& = (-1)^{2m} \begin{Bmatrix} c & j_i & a \\ j_i & m & 1 \end{Bmatrix} \text{Diagram} , \tag{3.17}
\end{aligned}$$

$$\begin{aligned}
& \text{Diagram} = (-1)^{j_j+m+b} (-1)^2 (-1)^{2m} \text{Diagram} = (-1)^{b+j_j-m} \begin{Bmatrix} d & j_j & b \\ j_j & m & 1 \end{Bmatrix} \text{Diagram} , \tag{3.18}
\end{aligned}$$

$$\begin{aligned}
\frac{c}{m} \frac{1}{m} \frac{d}{m} &= \frac{\delta_{c,d}}{d_d} \text{ (diagram with a circle and arrow) } = \frac{\delta_{c,d}}{d_d} (-1)^{m+1-c} \text{ (diagram with a triangle and arrow) } \\
&= \frac{\delta_{c,d}}{d_d} (-1)^{m+1-c} \left\{ \begin{matrix} c & m & 1 \\ 1 & 1 & m \end{matrix} \right\} \xrightarrow{c}, \tag{3.19}
\end{aligned}$$

in the second step, Eq. (2.13) in the third step, and Eqs. (2.12), (2.17)-(2.20) and (2.26) in the last step. Eq. (3.15) shows that the action of \hat{H}_v^E on ψ_i can be linearly expanded in terms of the normalized spin network states

$$\psi_t = \sqrt{d_{j_i} d_{j_j} d_{j_k} d_{j_l} d_a d_b d_m d_t} \cdot$$

In the definition of $\hat{H}_\delta^E(N)$ in [26], the spin m of arc a_{ij} was chosen in such a way that neither the spin a of e_i^1 nor the spin b of e_j^1 vanishes. Then the matrix elements $\langle \psi_i | \hat{H}_v^E | \psi_i \rangle$ can be easily calculated as

$$\begin{aligned}
\langle \psi_t | \hat{H}_{v, e_i, e_j}^E | \psi_i \rangle &= \chi(1) \chi(m) \chi(j_i) \chi(j_j) \sum_k \sqrt{d_k} \left(\widehat{V^{-1}}_v \right)_i^k d_a d_b \\
&\times \sum_c d_c (-1)^{b+c+j_j-1} \left\{ \begin{matrix} c & j_i & a \\ j_i & m & 1 \end{matrix} \right\} \left\{ \begin{matrix} c & j_j & b \\ j_j & m & 1 \end{matrix} \right\} \left\{ \begin{matrix} c & m & 1 \\ 1 & 1 & m \end{matrix} \right\} \\
&\times d_t (-1)^{j_l-j_i-k} (-1)^{t+b-j_k} \left\{ \begin{matrix} t & j_l & a \\ j_i & c & k \end{matrix} \right\} \left\{ \begin{matrix} t & j_k & b \\ j_j & c & k \end{matrix} \right\} \\
&\times \frac{1}{\sqrt{d_a d_b d_m d_t}}.
\end{aligned} \tag{3.21}$$

4 Relation in quantum dynamics

The quantum dynamics in covariant LQG is encoded in the partition function for a given SFM, while the quantum dynamics in canonical LQG is determined by the Hamiltonian constraint operator obtained from a suitable quantization procedure. To check the consistency of the two formulations of quantum dynamics is a crucial task. On one hand, in canonical LQG, one expects to construct the physical inner product in the physical Hilbert space by an antilinear rigging map [2]

$$\eta : \mathcal{D}_{\text{kin}} \rightarrow \mathcal{D}_{\text{phys}}^*; \quad \psi_s \mapsto \eta(\psi_s), \quad (4.1)$$

where \mathcal{D}_{kin} represents certain dense domain of \mathcal{H}_{kin} , and the space $\mathcal{D}_{\text{phys}}^*$ of solutions to the quantum Hamiltonian constraint is regarded as a subspace of the algebraic dual $\mathcal{D}_{\text{kin}}^*$ of \mathcal{D}_{kin} . Thus, the physical

inner product can be defined as

$$\langle \eta(\psi_s) | \eta(\psi_{s'}) \rangle_{\text{phys}} := [\eta(\psi_{s'})](\psi_s). \quad (4.2)$$

On the other hand, a SFM can naturally provide a rigging map by the transition amplitudes as

$$\langle \eta(\psi_s) | \eta(\psi_{s'}) \rangle_{\text{phys}} := \sum_{\partial \Delta^* = \psi_s \cup \psi_{s'}} \langle \psi_{s'} | \mathcal{Z}^{\text{SFM}}(\Delta^*) | \psi_s \rangle. \quad (4.3)$$

From the viewpoint of canonical LQG, the physical inner product should satisfy

$$\begin{aligned} \langle \hat{H}' \eta(\psi_s) | \eta(\psi_{s'}) \rangle_{\text{phys}} &= [\eta(\psi_{s'})](\hat{H} \psi_s) \\ &= \sum_{\partial \Delta^* = \hat{H} \psi_s \cup \psi_{s'}} \langle \psi_{s'} | \mathcal{Z}^{\text{SFM}}(\Delta^*) | \hat{H} \psi_s \rangle \\ &= \sum_{\partial \Delta^* = \psi_t \cup \psi_{s'}} \sum_{\psi_t} \langle \psi_{s'} | \mathcal{Z}^{\text{SFM}}(\Delta^*) | \psi_t \rangle \langle \psi_t | \hat{H} | \psi_s \rangle \\ &= 0, \end{aligned} \quad (4.4)$$

where \hat{H}' defined on $\mathcal{D}_{\text{kin}}^*$ is the dual of the Hamiltonian constraint operator \hat{H} defined on \mathcal{D}_{kin} . Eq. (4.4) implies the consistency between the covariant and canonical formulations of quantum dynamics in the sense that the Hamiltonian constraint of the latter is weakly satisfied for the physical states of the former.

We now check whether such a consistency exists between the covariant dynamics determined by Eq. (2.59) and the canonical dynamics given by Eq. (3.3). Let us consider the simple case in which Δ^* has only one internal vertex v , and focus on the Euclidean sector with the Immirzi parameter $\beta = 1$. Let ψ_s and $\psi_{s'}$ be two normalized gauge-invariant spin network states on a graph γ consisting of one vertex v_1 with possible different intertwiners and four edges e_1, \dots, e_4 starting from v_1 with the same spins on the same edges. By Eq. (3.10), Eq. (4.4) can be expressed as

$$\sum_{i, i'} f_s^i f_{s'}^{i'} \sum_{e_i \cap e_j = v} \sum_{\partial \Delta^* = \psi_t \cup \psi_{i'}} \sum_{\psi_t} \langle \psi_{i'} | \mathcal{Z}^{\text{EPRL}}(\Delta^*) | \psi_t \rangle \langle \psi_t | \hat{H}_{v, e_i, e_j}^E | \psi_i \rangle = 0, \quad (4.5)$$

where $\psi_{i'}$ is the normalized gauge-invariant spin network state with the same coupling scheme as that of ψ_i , but possible different intermediate coupling spins from that of ψ_i . It should be noted that only those ψ_t given by Eq. (3.20) have non-trivial contribution to the matrix elements of \hat{H}_{v, e_i, e_j}^E in (4.5). Note also that the partition function in Eq. (4.5) is defined on the Δ^* with some boundary states $\psi_{i'} \cup \psi_t$

and only one internal vertex v . The corresponding SFM can be graphically expressed by

where the orientations of faces agree with those of the edges of the boundary graphs of the spin network states, and we used Eq. (2.29) to reverse the orientations of edges in the initial state ψ_i and Eq. (2.19) to remove the arrows adding to the intertwiner at v_1 by reversing the orientations of edges. To see whether Eq. (4.5) is satisfied, it is sufficient to check whether one has equation

$$\sum_{\psi_t} \langle \psi_{t'} | \mathcal{Z}^{\text{EPRL}}(\Delta^*) | \psi_t \rangle \langle \psi_t | \hat{H}_{v, e_i, e_j}^E | \psi_i \rangle = 0. \quad (4.7)$$

Let us firstly compute the transition amplitude $\langle \psi_{t'} | \mathcal{Z}^{\text{EPRL}}(\Delta^*) | \psi_t \rangle$. By Eq. (2.43), the condition $\beta = 1$ implies

$$j_f^+ = j_f = j_l, \quad j_f^- = 0, \quad \forall l \in \partial\Delta^* \cap f. \quad (4.8)$$

This condition simplifies the fusion functions $f_{i_e^+ i_e^-}^{i_e}$ as well as the vertex amplitudes in the transition amplitude (2.62). For example, the fusion function associated to the internal edge linking v and v_2 reads

where Eqs. (2.5), (2.19), (2.14) and (2.15) were used. The vertex amplitude A_v associated to the

internal vertex v is reduced to

$$\begin{aligned}
A_v &= \text{Tr}(i_{v_1} \otimes i_{v_2} \otimes i_{v_3} \otimes i_{v_4}) = j_l \text{ (diagram)} j_k = \sqrt{d_t d_{i'}} j_l \text{ (diagram)} j_k \\
&= \sqrt{d_t d_{i'}} (-1)^{i'+j_l-j_l} (-1)^{a+m+j_i} (-1)^{i'+j_j+j_k} (-1)^{b+m+j_j} (-1)^{t+m+i'} \begin{Bmatrix} j_i & m & a \\ t & j_l & i' \end{Bmatrix} \begin{Bmatrix} j_j & m & b \\ t & j_k & i' \end{Bmatrix}, \quad (4.10)
\end{aligned}$$

where we used Eq. (2.23) in the third step, and the identity

$$\begin{aligned}
&\text{(diagram)} + \text{(diagram)} \\
&= (-1)^{i'+j_l-j_l} (-1)^{a+m+j_i} \text{(diagram)} + (-1)^{i'+j_j+j_k} (-1)^{b+m+j_j} (-1)^{t+m+i'} \text{(diagram)} \\
&= (-1)^{i'+j_l-j_l} (-1)^{a+m+j_i} (-1)^{i'+j_j+j_k} (-1)^{b+m+j_j} (-1)^{t+m+i'} \begin{Bmatrix} j_i & m & a \\ t & j_l & i' \end{Bmatrix} \begin{Bmatrix} j_j & m & b \\ t & j_k & i' \end{Bmatrix}, \quad (4.11)
\end{aligned}$$

in the last step. Thus, the transition amplitude between $\psi_{i'}$ and ψ_t defined in Eq. (2.62) can be calculated as

$$\begin{aligned}
\langle \psi_{i'} | \mathcal{Z}^{\text{EPRL}}(\Delta^*) | \psi_t \rangle &= d_{j_i} d_{j_j} d_{j_k} d_{j_l} d_a d_b d_m j_l \text{ (diagram)} j_k \times \frac{1}{d_{j_i} d_{j_j} d_{j_k} d_{j_l} \sqrt{d_a d_b d_m}} \\
&= \sqrt{d_a d_b d_m} \sqrt{d_t d_{i'}} (-1)^{i'+j_l-j_l} (-1)^{a+m+j_i} (-1)^{i'+j_j+j_k} (-1)^{b+m+j_j} (-1)^{t+m+i'} \\
&\quad \times \begin{Bmatrix} j_i & m & a \\ t & j_l & i' \end{Bmatrix} \begin{Bmatrix} j_j & m & b \\ t & j_k & i' \end{Bmatrix}. \quad (4.12)
\end{aligned}$$

Combining Eqs. (4.12) and (3.21) yields

$$\begin{aligned}
& \sum_{\psi_t} \langle \psi_{i'} | \mathcal{Z}^{\text{EPRL}}(\Delta^*) | \psi_t \rangle \langle \psi_t | \hat{H}_{v, e_i, e_j}^E | \psi_i \rangle \\
&= \sqrt{d_{i'}} \chi(1) \chi(m) \chi(j_i) \chi(j_j) \sum_k \sqrt{d_k} \left(\widehat{V^{-1}}_v \right)_i^k \sum_{c,t} d_t d_c (-1)^{c-i'-m+2t+k-j_i-j_j-j_k-j_l-1} \left\{ \begin{matrix} c & m & 1 \\ 1 & 1 & m \end{matrix} \right\} \\
&\quad \times \sum_a (-1)^{R_a} d_a \left\{ \begin{matrix} c & j_i & a \\ j_i & m & 1 \end{matrix} \right\} \left\{ \begin{matrix} j_i & m & a \\ t & j_l & i' \end{matrix} \right\} \left\{ \begin{matrix} t & j_l & a \\ j_i & c & k \end{matrix} \right\} \sum_b (-1)^{R_b} d_b \left\{ \begin{matrix} c & j_j & b \\ j_j & m & 1 \end{matrix} \right\} \left\{ \begin{matrix} j_j & m & b \\ t & j_k & i' \end{matrix} \right\} \left\{ \begin{matrix} t & j_k & b \\ j_j & c & k \end{matrix} \right\} \\
&= \sqrt{d_{i'}} \chi(1) \chi(m) \chi(j_i) \chi(j_j) (-1)^{i'+m-j_i-j_j-j_k-j_l} \sum_k \sqrt{d_k} \left(\widehat{V^{-1}}_v \right)_i^k \left\{ \begin{matrix} 1 & i' & k \\ j_l & j_i & j_i \end{matrix} \right\} \left\{ \begin{matrix} 1 & i' & k \\ j_k & j_i & j_i \end{matrix} \right\} \\
&\quad \times \sum_t d_t (-1)^t \sum_c (-1)^{R_c} d_c \left\{ \begin{matrix} 1 & m & c \\ t & k & i' \end{matrix} \right\} \left\{ \begin{matrix} t & k & c \\ 1 & m & i' \end{matrix} \right\} \left\{ \begin{matrix} 1 & m & c \\ m & 1 & 1 \end{matrix} \right\} \\
&= \sqrt{d_{i'}} \chi(1) \chi(m) \chi(j_i) \chi(j_j) (-1)^{i'+m-j_i-j_j-j_k-j_l} \\
&\quad \times \sum_k \sqrt{d_k} \left(\widehat{V^{-1}}_v \right)_i^k \left\{ \begin{matrix} 1 & i' & k \\ j_l & j_i & j_i \end{matrix} \right\} \left\{ \begin{matrix} 1 & i' & k \\ j_k & j_i & j_i \end{matrix} \right\} \left\{ \begin{matrix} i' & i' & 1 \\ 1 & 1 & k \end{matrix} \right\} \sum_t d_t (-1)^t \left\{ \begin{matrix} i' & i' & 1 \\ m & m & t \end{matrix} \right\} \\
&= 0,
\end{aligned} \tag{4.13}$$

where in the second and third steps we used [49, 50]

$$\sum_x (-1)^{R_x} d_x \left\{ \begin{matrix} a & b & x \\ c & d & p \end{matrix} \right\} \left\{ \begin{matrix} c & d & x \\ e & f & q \end{matrix} \right\} \left\{ \begin{matrix} e & f & x \\ b & a & r \end{matrix} \right\} = \left\{ \begin{matrix} p & q & r \\ e & a & d \end{matrix} \right\} \left\{ \begin{matrix} p & q & r \\ f & b & c \end{matrix} \right\} \tag{4.14}$$

with

$$R_x := a + b + c + d + e + f + p + q + r + x, \tag{4.15}$$

and in the last step we used [49]

$$\sum_x d_x (-1)^x \left\{ \begin{matrix} j_1 & j_1 & j_3 \\ l_1 & l_1 & x \end{matrix} \right\} = (-1)^{-j_1-l_1} \sqrt{d_{j_1} d_{l_1}} \delta_{j_3,0}. \tag{4.16}$$

Hence Eq. (4.7) is satisfied for the graph γ with a 4-valent vertex. The above calculations can be easily generalized to the case that a graph γ has a vertex with valence more than four. In this general case, the states appeared in Eq. (4.7) can be graphically expressed by

$$\psi_i = f_i \begin{array}{c} \begin{array}{ccccccc} & + & & + & & + & & + \\ & \xrightarrow{\quad} & & \xrightarrow{\quad} & & \xrightarrow{\quad} & & \xrightarrow{\quad} \\ e_n \downarrow & j_m & e_n \downarrow & j_n & e_l \downarrow & j_l & e_i \downarrow & j_i & e_j \downarrow & j_j & e_k \downarrow & j_k & e_s \downarrow & j_s & e_t \downarrow & j_t \end{array} \end{array}, \tag{4.17}$$

$$\psi_t = f_t \begin{array}{c} \begin{array}{ccccccc} & + & & + & & + & & + \\ & \xrightarrow{\quad} & & \xrightarrow{\quad} & & \xrightarrow{\quad} & & \xrightarrow{\quad} \\ e_n \downarrow & j_m & e_n \downarrow & j_n & e_l \downarrow & j_l & e_i \downarrow & j_i & e_j \downarrow & j_j & e_k \downarrow & j_k & e_s \downarrow & j_s & e_t \downarrow & j_t \end{array} \end{array}, \tag{4.18}$$

$$\psi_{i'} = f_{i'} \begin{array}{c} \text{---} \xrightarrow{+} \text{---} \xrightarrow{a'_l} \text{---} \xrightarrow{i'} \text{---} \xrightarrow{a'_k} \text{---} \xrightarrow{+} \text{---} \\ \downarrow e_m j_m \quad \downarrow e_n j_n \quad \downarrow e_l j_l \quad \downarrow e_i j_i \quad \downarrow j_j e_j \quad \downarrow e_k j_k \quad \downarrow e_s j_s \quad \downarrow e_t j_t \\ \text{---} \end{array}, \quad (4.19)$$

where $f_i, f_t, f_{i'}$ denote the normalized factors. Then the transition amplitude between $\psi_{i'}$ and ψ_t defined in Eq. (2.62) can be calculated as

$$\begin{aligned} \langle \psi_{i'} | \mathcal{Z}^{\text{EPRL}}(\Delta^*) | \psi_t \rangle &= \sqrt{d_a d_b d_m} \sqrt{\prod_x d_{a'_x} d_t} \sqrt{\prod_y d_{a''_y} d_{i'}} \begin{array}{c} \text{---} \xrightarrow{+} \text{---} \xrightarrow{a''_l} \text{---} \xrightarrow{t} \text{---} \xrightarrow{a''_k} \text{---} \xrightarrow{+} \text{---} \\ \downarrow j_m \quad \downarrow j_n \quad \downarrow j_l \quad \downarrow a \quad \downarrow b \quad \downarrow j_k \quad \downarrow j_s \quad \downarrow j_t \\ \text{---} \end{array} \\ &= \left(\prod_x \delta_{a'_x, a''_x} \right) \sqrt{d_a d_b d_m} a'_l \begin{array}{c} \text{---} \xrightarrow{+} \text{---} \xrightarrow{t} \text{---} \xrightarrow{+} \text{---} \\ \downarrow \sqrt{d_t} \quad \downarrow a \quad \downarrow b \quad \downarrow \sqrt{d_t} \\ \downarrow j_l \quad \downarrow m \quad \downarrow j_k \\ \downarrow j_i \quad \downarrow j_j \\ \downarrow \sqrt{d_{i'}} \quad \downarrow i' \quad \downarrow \sqrt{d_{i'}} \\ \text{---} \end{array} \\ &= \left(\prod_x \delta_{a'_x, a''_x} \right) \sqrt{d_a d_b d_m} \sqrt{d_t d_{i'}} (-1)^{i' + j_i - a'_l} (-1)^{a + m + j_i} (-1)^{i' + j_j + a'_k} \\ &\quad \times (-1)^{b + m + j_j} (-1)^{t + m + i'} \begin{Bmatrix} j_i & m & a \\ t & a'_l & i' \end{Bmatrix} \begin{Bmatrix} j_j & m & b \\ t & a'_k & i' \end{Bmatrix}, \quad (4.20) \end{aligned}$$

where we used Eqs. (2.14) and (2.19) in the second step, and Eq. (4.10) in the third step. In this case, the matrix element $\langle \psi_t | \hat{H}_{v, e_i, e_j}^E | \psi_i \rangle$ reads

$$\begin{aligned} \langle \psi_t | \hat{H}_{v, e_i, e_j}^E | \psi_i \rangle &= \chi(1) \chi(m) \chi(j_i) \chi(j_j) \sum_{\vec{d}'', k} \sqrt{d_k} \langle \vec{d}'', k | \widehat{V}^{-1}_v | \vec{d}, i \rangle d_a d_b \\ &\quad \times \sum_c d_c (-1)^{b + c + j_j - 1} \begin{Bmatrix} c & j_i & a \\ j_i & m & 1 \end{Bmatrix} \begin{Bmatrix} c & j_j & b \\ j_j & m & 1 \end{Bmatrix} \begin{Bmatrix} c & m & 1 \\ 1 & 1 & m \end{Bmatrix} \\ &\quad \times d_t (-1)^{a'_l - j_i - k} (-1)^{t + b - a'_k} \begin{Bmatrix} t & a''_l & a \\ j_i & c & k \end{Bmatrix} \begin{Bmatrix} t & a''_k & b \\ j_j & c & k \end{Bmatrix} \\ &\quad \times \frac{1}{\sqrt{d_a d_b d_m d_t}}, \quad (4.21) \end{aligned}$$

where $|\vec{d}, i\rangle$ denotes the normalized intertwiner of ψ_i in Eq. (4.17), \vec{d} denotes the set of intermediate coupling spins other than i , and $|\vec{d}'', k\rangle$ is the one obtained from $|\vec{d}, i\rangle$ by replacing \vec{d} by \vec{d}'' and i by k .

Combining Eqs. (4.20) and (4.21), we have

$$\begin{aligned}
& \sum_{\psi_t} \langle \psi_{i'} | \mathcal{Z}^{\text{EPRL}}(\Delta^*) | \psi_t \rangle \langle \psi_t | \hat{H}_{v,e_i,e_j}^E | \psi_i \rangle \\
&= \sqrt{d_{i'}} \chi(1) \chi(m) \chi(j_i) \chi(j_j) \sum_k \sqrt{d_k} \left\langle \vec{d}', k \left| \widehat{V^{-1}}_v \right| \vec{d}, i \right\rangle \sum_{c,t} d_t d_c (-1)^{c-i'-m+2t+k-j_i-j_j-a'_k-a'_l-1} \begin{Bmatrix} c & m & 1 \\ 1 & 1 & m \end{Bmatrix} \\
&\quad \times \sum_a (-1)^{R_a} d_a \begin{Bmatrix} c & j_i & a \\ j_i & m & 1 \end{Bmatrix} \begin{Bmatrix} j_i & m & a \\ t & a'_l & i' \end{Bmatrix} \begin{Bmatrix} t & a'_l & a \\ j_i & c & k \end{Bmatrix} \sum_b (-1)^{R_b} d_b \begin{Bmatrix} c & j_j & b \\ j_j & m & 1 \end{Bmatrix} \begin{Bmatrix} j_j & m & b \\ t & a'_k & i' \end{Bmatrix} \begin{Bmatrix} t & a'_k & b \\ j_j & c & k \end{Bmatrix} \\
&= 0.
\end{aligned} \tag{4.22}$$

Therefore, in the general case, the quantum dynamics between the covariant and canonical LQG, determined by the generalized Euclidean EPRL model and by the Hamiltonian constraint operator $\hat{H}_\delta^E(N)$ respectively, are consistent to each other on the spin network states with one vertex in the sense of Eq. (4.4) for $\beta = 1$.

5 Summary and discussion

A major challenge in LQG is how to relate its covariant formulation to its canonical formulation in quantum dynamics. In previous sections, we studied the relation by taking the viewpoint that SFM provides a rigging map such that the Hamiltonian constraint in canonical LQG is weakly satisfied. This idea was first proposed in [32], where the consistency between the EPRL SFM and the Euclidean Hamiltonian constraint operator proposed by Thiemann in [24] was checked. While the same EPRL SFM is concerned here, the Hamiltonian constraint operator which we considered is the Euclidean version $\hat{H}^E(N)$ proposed in [26]. The virtue of $\hat{H}^E(N)$ is that it is well defined in certain partially diffeomorphism invariant Hilbert space and can be promoted to a symmetric operator.

The graphical calculus was used as a powerful tool to give direct and concise derivations of the partition function $\mathcal{Z}^{\text{EPRL}}(\Delta^*)$ in Eqs. (2.50) (or (2.53)) and (2.59) (or (2.61)) of generalized Euclidean EPRL model for Δ^* without and with a boundary respectively, as well as the matrix elements (3.21) (or Eq. (4.21)) of the Hamiltonian constraint operator $\hat{H}_\delta^E(N)$ on certain spin network states. Our result of Eq. (4.22) shows that in the Euclidean case the generalized EPRL model can provide a rigging map such that the Hamiltonian constraint operator proposed in [26] is weakly satisfied on the spin network states with one vertex for the Immirzi parameter $\beta = 1$. Hence, in this sense, the quantum dynamics between covariant LQG and canonical LQG are consistent to each other for these states. Moreover, we showed how to generalize the graphical calculus to the calculations of SFMs. It provides a visual and powerful tool alternative to the algebraic one.

It should be noted that the Hamiltonian constraint operator $\hat{H}^E(N)$ is well defined in the Hilbert space \mathcal{H}_{np4} consisting of the almost diffeomorphism invariant states obtained by group-averaging the diffeomorphisms of Σ but leaving fixed sets of non-planar vertices with valence higher than 3 invariant. Though the results of Eqs. (4.13) and (4.22) were derived with the kinematical Hilbert space \mathcal{H}_{kin} , there is no obstacle to promote them to \mathcal{H}_{np4} since the partially diffeomorphism transformations neither change the relevant vertices nor change the intertwiners and spins on the graphs. Hence, our

results indicate actually the consistency between the partially diffeomorphism invariant generalized EPRL SFM and $\hat{H}^E(N)$ in \mathcal{H}_{np4} of canonical LQG. The fact that the rigging map given by the EPRL SFM can weakly satisfy both Thiemann's Hamiltonian $\hat{H}_T^E(N)$ in [24] and the Hamiltonian constraint $\hat{H}^E(N)$ in [26] manifests that the physical states provided by the rigging map on the spin network states with one vertex does not include all the solutions to $\hat{H}_T^E(N)$ or $\hat{H}^E(N)$. Further investigation are still desirable to reveal more accurate relations between the covariant and canonical dynamics of LQG.

Acknowledgments

This work is supported in part by NSFC Grants No. 11765006, No. 11961131013 and No. 11875006. C. Z. acknowledges the support by the Polish Narodowe Centrum Nauki, Grant No. 2018/30/Q/ST2/00811.

References

- [1] C. Rovelli, *Quantum Gravity*. Cambridge University Press, Cambridge, United Kingdom, 2004, [10.1017/CBO9780511755804](#).
- [2] T. Thiemann, *Modern Canonical Quantum General Relativity*. Cambridge University Press, Cambridge, England, 2007, [10.1017/CBO9780511755682](#).
- [3] *Loop Quantum Gravity: The First 30 Years*, edited by A. Ashtekar and J. Pullin, World Scientific, Singapore, 2017.
- [4] T. Thiemann, *Lectures on loop quantum gravity*, *Lect. Notes Phys.* **631** (2003) 41 [[gr-qc/0210094](#)].
- [5] A. Ashtekar and J. Lewandowski, *Background independent quantum gravity: A status report*, *Class. Quant. Grav.* **21** (2004) R53 [[gr-qc/0404018](#)].
- [6] M. Han, Y. Ma and W. Huang, *Fundamental structure of loop quantum gravity*, *Int. J. Mod. Phys. D* **16** (2007) 1397 [[gr-qc/0509064](#)].
- [7] K. Giesel and H. Sahlmann, *From classical to quantum gravity: Introduction to loop quantum gravity*, *Proc. Sci.* **QGQS2011** (2011) 002 [[1203.2733](#)].
- [8] J. C. Baez, *An introduction to spin foam models of quantum gravity and BF theory*, *Lect. Notes Phys.* **543** (2000) 25 [[gr-qc/9905087](#)].
- [9] C. Rovelli, *Zakopane lectures on loop gravity*, *PoS QGQS2011* (2011) 003 [[1102.3660](#)].
- [10] A. Perez, *The spin-foam approach to quantum gravity*, *Living Rev. Rel.* **16** (2013) 3 [[1205.2019](#)].
- [11] A. Ashtekar, *New variables for classical and quantum gravity*, *Phys. Rev. Lett.* **57** (1986) 2244.
- [12] A. Ashtekar, *New Hamiltonian formulation of general relativity*, *Phys. Rev. D* **36** (1987) 1587.
- [13] J. F. Barbero, *Real Ashtekar variables for Lorentzian signature space-times*, *Phys. Rev. D* **51** (1995) 5507 [[gr-qc/9410014](#)].
- [14] G. Immirzi, *Quantum gravity and Regge calculus*, *Nucl. Phys. B - Proc. Suppl.* **57** (1997) 65 [[gr-qc/9701052](#)].

- [15] J. Lewandowski, A. Okołów, H. Sahlmann and T. Thiemann, *Uniqueness of diffeomorphism invariant states on holonomy–flux algebras*, *Commun. Math. Phys.* **267** (2006) 703 [[gr-qc/0504147](#)].
- [16] A. Ashtekar and C. J. Isham, *Representations of the holonomy algebras of gravity and nonAbelian gauge theories*, *Class. Quant. Grav.* **9** (1992) 1433 [[hep-th/9202053](#)].
- [17] A. Ashtekar and J. Lewandowski, *Projective techniques and functional integration for gauge theories*, *J. Math. Phys.* **36** (1995) 2170 [[gr-qc/9411046](#)].
- [18] C. Rovelli and L. Smolin, *Discreteness of area and volume in quantum gravity*, *Nucl. Phys. B* **442** (1995) 593 [[gr-qc/9411005](#)].
- [19] A. Ashtekar and J. Lewandowski, *Quantum theory of geometry: I. Area operators*, *Class. Quant. Grav.* **14** (1997) A55 [[gr-qc/9602046](#)].
- [20] A. Ashtekar and J. Lewandowski, *Quantum theory of geometry II: Volume operators*, *Adv. Theor. Math. Phys.* **1** (1997) 388 [[gr-qc/9711031](#)].
- [21] J. Yang and Y. Ma, *New volume and inverse volume operators for loop quantum gravity*, *Phys. Rev. D* **94** (2016) 044003 [[1602.08688](#)].
- [22] T. Thiemann, *A length operator for canonical quantum gravity*, *J. Math. Phys.* **39** (1998) 3372 [[gr-qc/9606092](#)].
- [23] Y. Ma, C. Soo and J. Yang, *New length operator for loop quantum gravity*, *Phys. Rev. D* **81** (2010) 124026 [[1004.1063](#)].
- [24] T. Thiemann, *Quantum spin dynamics (QSD)*, *Class. Quant. Grav.* **15** (1998) 839 [[gr-qc/9606089](#)].
- [25] T. Thiemann, *Quantum spin dynamics (QSD): V. Quantum gravity as the natural regulator of matter quantum field theories*, *Class. Quant. Grav.* **15** (1998) 1281 [[gr-qc/9705019](#)].
- [26] J. Yang and Y. Ma, *New Hamiltonian constraint operator for loop quantum gravity*, *Phys. Lett. B* **751** (2015) 343 [[1507.00986](#)].
- [27] E. Alesci, M. Assanioussi, J. Lewandowski and I. Mäkinen, *Hamiltonian operator for loop quantum gravity coupled to a scalar field*, *Phys. Rev. D* **91** (2015) 124067 [[1504.02068](#)].
- [28] C. Tomlin and M. Varadarajan, *Towards an anomaly-free quantum dynamics for a weak coupling limit of Euclidean gravity*, *Phys. Rev. D* **87** (2013) 044039 [[1210.6869](#)].
- [29] C. Tomlin and M. Varadarajan, *Towards an anomaly-free quantum dynamics for a weak coupling limit of Euclidean gravity: Diffeomorphism covariance*, *Phys. Rev. D* **87** (2013) 044040 [[1210.6877](#)].
- [30] M. Varadarajan, *Constraint algebra in Smolin’s $G \rightarrow 0$ limit of 4d Euclidean gravity*, *Phys. Rev. D* **97** (2018) 106007 [[1802.07033](#)].
- [31] M. Varadarajan, *Quantum propagation in Smolin’s weak coupling limit of 4D Euclidean gravity*, *Phys. Rev. D* **100** (2019) 066018 [[1904.02247](#)].
- [32] E. Alesci, T. Thiemann and A. Zipfel, *Linking covariant and canonical LQG: New solutions to the Euclidean scalar constraint*, *Phys. Rev. D* **86** (2012) 024017 [[1109.1290](#)].
- [33] T. Thiemann and A. Zipfel, *Linking covariant and canonical LQG II: Spin foam projector*, *Class. Quant. Grav.* **31** (2014) 125008 [[1307.5885](#)].
- [34] C. Zhang, J. Lewandowski and Y. Ma, *Towards the self-adjointness of a Hamiltonian operator in loop quantum gravity*, *Phys. Rev. D* **98** (2018) 086014 [[1805.08644](#)].

- [35] C. Zhang, J. Lewandowski, H. Li and Y. Ma, *Bouncing evolution in a model of loop quantum gravity*, *Phys. Rev. D* **99** (2019) 124012 [[1904.07046](#)].
- [36] J. W. Barrett and L. Crane, *Relativistic spin networks and quantum gravity*, *J. Math. Phys.* **39** (1998) 3296 [[gr-qc/9709028](#)].
- [37] J. W. Barrett and L. Crane, *A Lorentzian signature model for quantum general relativity*, *Class. Quant. Grav.* **17** (2000) 3101 [[gr-qc/9904025](#)].
- [38] J. Engle, E. Livine, R. Pereira and C. Rovelli, *LQG vertex with finite Immirzi parameter*, *Nucl. Phys. B* **799** (2008) 136 [[0711.0146](#)].
- [39] L. Freidel and K. Krasnov, *A new spin foam model for 4d gravity*, *Class. Quant. Grav.* **25** (2008) 125018 [[0708.1595](#)].
- [40] Y. Ding and C. Rovelli, *The volume operator in covariant quantum gravity*, *Class. Quant. Grav.* **27** (2010) 165003 [[0911.0543](#)].
- [41] E. R. Livine and S. Speziale, *A new spinfoam vertex for quantum gravity*, *Phys. Rev. D* **76** (2007) 084028 [[0705.0674](#)].
- [42] W. Kamiński, M. Kisielowski and J. Lewandowski, *Spin-foams for all loop quantum gravity*, *Class. Quant. Grav.* **27** (2010) 095006 [[0909.0939](#)].
- [43] Y. Ding, M. Han and C. Rovelli, *Generalized spinfoams*, *Phys. Rev. D* **83** (2011) 124020 [[1011.2149](#)].
- [44] J. Yang and Y. Ma, *Graphical calculus of volume, inverse volume and Hamiltonian operators in loop quantum gravity*, *Eur. Phys. J. C* **77** (2017) 235 [[1505.00223](#)].
- [45] D. M. Brink and G. R. Satchler, *Angular Momentum*. Clarendon Press, 1968.
- [46] J. Yang and Y. Ma, *Consistency check on the fundamental and alternative flux operators in loop quantum gravity*, *Chin. Phys. C* **43** (2019) 103106 [[1908.10600](#)].
- [47] C. P. Rourke and B. J. Sanderson, *Introduction to Piecewise-Linear Topology*. Berlin, Springer, 1972.
- [48] J. Engle and R. Pereira, *Coherent states, constraint classes, and area operators in the new spin-foam models*, *Class. Quant. Grav.* **25** (2008) 105010 [[0710.5017](#)].
- [49] A. P. Yutsis, I. B. Levinson and V. V. Vanagas, *Mathematical Apparatus of the Theory of Angular Momentum*. Israel Program for Scientific Translations, Translated from Russian by A. Sen and R. N. Sen, 1962.
- [50] D. A. Varshalovich, A. N. Moskalev and V. K. Khersonsky, *Quantum Theory of Angular Momentum: Irreducible Tensors, Spherical Harmonics, Vector Coupling Coefficients, 3nj Symbols*. World Scientific, Singapore, 1988.